UNIVERSITY OF TURKU

Harnessing pathologic depression through allosteric modulation of neuronal plasticity receptors

Enabling neuroplasticity with psychedelics

Institute of Biomedicine
MDP in Drug Discovery and Development
Master's thesis

Author:
Riikka Isotalo

Supervisors:
Vadim Le Joncour, Ph.D., Doc., University of Helsinki
Eero Castrén, M.D., Ph.D., Research Director, University of Helsinki

15.05.2025
Turku

I hereby declare that generative artificial intelligence was used as a supportive tool in the preparation of this thesis. The work remains entirely my own, and I am fully responsible for all content. Details of the tools used and their specific applications are provided in Appendix 1

The originality of this thesis has been checked in accordance with the University of Turku quality assurance system using the Turnitin Originality Check service.

Master's thesis

Subject: Institute of Biomedicine, MDP in Biomedical Sciences, Drug Discovery and Development

Author: Riikka Isotalo

Title: Harnessing pathologic depression through allosteric modulation of neuronal plasticity receptors

Supervisors: Docent Vadim Le Joncour
Neuroscience Center, Helsinki Institute of Life Science HiLIFE,
University of Helsinki

Research Director Eero Castrén
Neuroscience Center, Helsinki Institute of Life Science HiLIFE,
University of Helsinki

Number of pages and appendices: 49 pages, 1 appendix

Date: 15.05.2026

Depression is a major global health burden, and currently available antidepressants are limited by delayed therapeutic onset and incomplete efficacy. Increasing evidence suggests that antidepressant effects are mediated not only through monoaminergic neurotransmission but also through enhancement of neuronal plasticity involving brain-derived neurotrophic factor (BDNF) and its receptor tropomyosin receptor kinase B (TrkB). Recent studies have further proposed that psychedelics may directly interact with TrkB and modulate neuroplasticity-related signaling pathways.

The aim of this study was to establish and optimize assay procedures for the newly introduced Dianthus affinity screening platform for investigation of ligand-TrkB interactions in TrkB-expressing cell lysates, and to perform preliminary evaluation of selected ligands. TrkB abundance and molecular heterogeneity were characterized using Western blotting and ELISA, while receptor glycosylation state was investigated with brefeldin A treatment.

The results demonstrated that assay performance was highly dependent on sample preparation. Multiple TrkB-immunoreactive bands consistent with heterogeneous receptor populations and distinct glycosylation states were observed. Preliminary concentration-dependent responses associated with lysergic acid diethylamide (LSD) were detected in TrkB-containing lysates. Together, these findings provide methodological groundwork for future quantitative studies investigating TrkB-targeting antidepressant and psychedelic compounds.

Key words: neuroplasticity, TrkB, Dianthus

Table of contents

1 Introduction

1.1 Depression as a global health burden and the unmet need for novel therapies

Depression, more precisely major depressive disorder or clinical depression, is one of the leading causes of disability worldwide and has posed a significant public health burden for over three decades (GBD 2019 Mental Disorders Collaborators, 2022). This burden has been further exacerbated by the COVID-19 pandemic, which has substantially increased the prevalence and severity of mental health issues globally (Santomauro et al., 2021). In addition to its high prevalence, affecting nearly 300 million people globally, the pathophysiology of depression is still not fully understood, it is associated with substantial personal, social and economic costs and it commonly co-occurs with other psychiatric and somatic conditions such as anxiety disorders, sleep disturbances, and substance use disorders (GBD 2019 Mental Disorders Collaborators, 2022; Malhi & Mann, 2018). Together, these factors make depression a highly heterogenous and clinically challenging disorder.

Although several antidepressant drugs are widely available, current treatments remain far from optimal. Their limitations include modest efficacy, delayed onset of therapeutic effects, low remission rates, frequent adverse effects, substantial variability in response, and poor long-term outcomes (Cipriani et al., 2018; Rush et al., 2006). STAR*D study and more recent analyses of treatment-resistant depression treatment outcomes have shown that nearly two-thirds of patients fail to achieve remission with first-line treatment, and many remain symptomatic even after multiple treatment attempts (Rush et al., 2006; Saelens et al., 2025). These findings highlight not only the limitations of current therapies but also the urgent need for novel and mechanistically distinct antidepressant strategies (Malhi & Mann, 2018; Mulinari, 2012).

The majority of conventional antidepressants share a common mechanism of action: they modulate monoaminergic neurotransmission, particularly by increasing the synaptic availability of primarily serotonin, noradrenaline, and dopamine (Hirschfeld, 2000; Malhi & Mann, 2018; Nestler et al., 2002). While these drugs are clinically beneficial, their limitations have increasingly raised questions whether monoamine-centered models are sufficient to explain either the pathophysiology of depression or the mechanism of

antidepressant action. This has led to growing interest in alternative frameworks that focus on the neurobiological processes underlying stress adaptation and circuit-level dysfunction.

1.2 From the monoamine hypothesis to the neuroplasticity hypothesis of depression

The monoamine hypothesis has historically been highly influential model of depression being the cornerstone of antidepressant drug development for over half a century (Hirschfeld, 2000; Mulinari, 2012). According to this theory the underlying cause of depression is monoamine deficiency in the central nervous system (CNS). This concept of "chemical imbalance" due to depletion of these neurotransmitters provided a pharmacologically convenient explanation for antidepressant action still forming the basis of current treatment which consists mainly of serotonergic antidepressants such as selective serotonin reuptake inhibitors (SSRIs).

However, the explanatory power of the monoamine hypothesis is limited. Most importantly, it does not adequately explain the delay between acute pharmacological effects and relevant clinical improvement (Hirschfeld, 2000; Nestler et al., 2002). Monoamine levels increase within hours after antidepressant administration, whereas symptom relief usually emerges after weeks of continuous treatment. Nor does the monoamine hypothesis explain the modest response and remission rates (Cipriani et al., 2018; Harmer et al., 2017; Rush et al., 2006).

These shortcomings have contributed to a broader theoretical shift. Rather than viewing depression primarily as a disorder of acute neurotransmitter levels it is increasingly considered as one of impaired neuroplasticity, maladaptive stress responses and malfunctioning neural circuits (Albert, 2019; Castrén, 2005; Kraus et al., 2017; Liu et al., 2017; Manji et al., 2001). In this framework, antidepressants are not seen only as modulators of monoamine levels but as agents that promote plasticity further enabling the remodeling of the dysfunctional neural networks over time.

1.3 Neuroplasticity in depression: stress, maladaptation, and reversal by antidepressants

Neuroplasticity refers to the brain's ability to reorganize its structure, function, and connections in response to intrinsic and extrinsic stimuli. It is a fundamental property of the

nervous system and is essential for learning, memory, emotional adaptation and behavioral flexibility (Park & Poo, 2013; Wang et al., 2022). In healthy brain, neuroplasticity supports both developmental processes and adaptive responses throughout life.

In depression, however, these mechanisms appear to be disrupted (Nestler et al., 2002; Fuchs and Flügge, 2014; Malhi & Mann, 2018; Wang et al., 2022). Chronic stress, one of the strongest risk factors for depression, has been shown to impair both structural and functional plasticity, particularly in brain regions involved in mood regulation such as the hippocampus and prefrontal cortex (Duman & Monteggia, 2006; Duman et al., 2016; Pittenger & Duman, 2008). These changes include dendritic atrophy, reduced spine density, altered synaptic strength, and impaired neurogenesis, all of which may contribute to persistent depressive symptoms and cognitive deficits.

Importantly, these alterations are not merely downstream consequences of depression but are thought to play a central role in its pathophysiology. This has led to the neuroplasticity hypothesis of depression, which proposes that depression is associated with reduced capacity of neuronal circuits to adapt and reorganize appropriately (Albert, 2019; Castrén, 2005). In line with this view, effective antidepressant treatments restore or facilitate plasticity in malfunctioning neural networks.

Supporting this framework, antidepressant treatments have been shown to reverse many of the stress-induced deficits observed in preclinical models (Duman & Monteggia, 2006; Duman et al., 2016; Pittenger & Duman, 2008). Antidepressants appear to promote synaptic remodeling and neuronal survival improving network function rather than solely acting through acute changes in monoamine levels.

1.4 BDNF/TrkB signalling in neuronal plasticity and mood disorders

Among the molecular regulators of neuroplasticity, brain-derived neurotrophic factor (BDNF) and its high-affinity receptor neuronal receptor tyrosine kinase 2 (TrkB, or NTRK2) have emerged as central components in both normal brain function and the pathophysiology of depression (Autry & Monteggia, 2012; Castrén & Monteggia, 2021; Huang & Reichardt, 2001; Park & Poo, 2013; Wang et al., 2022). BDNF is a neurotrophin that plays a critical role in neuronal survival, differentiation, and synaptic plasticity, while TrkB mediates its downstream effects through activation of intracellular signaling pathways.

TrkB is a single-pass transmembrane receptor tyrosine kinase consisting of an extracellular ligand-binding domain (ECD), a transmembrane domain (TMD), and an intracellular kinase domain (KD) (Enkavi et al., 2024; Huang & Reichardt, 2003). The overall domain organization is illustrated in Figure 1A. The ECD mediates binding of endogenous neurotrophins such as BDNF, whereas the KD is responsible for downstream signaling through phosphorylation-dependent pathways.

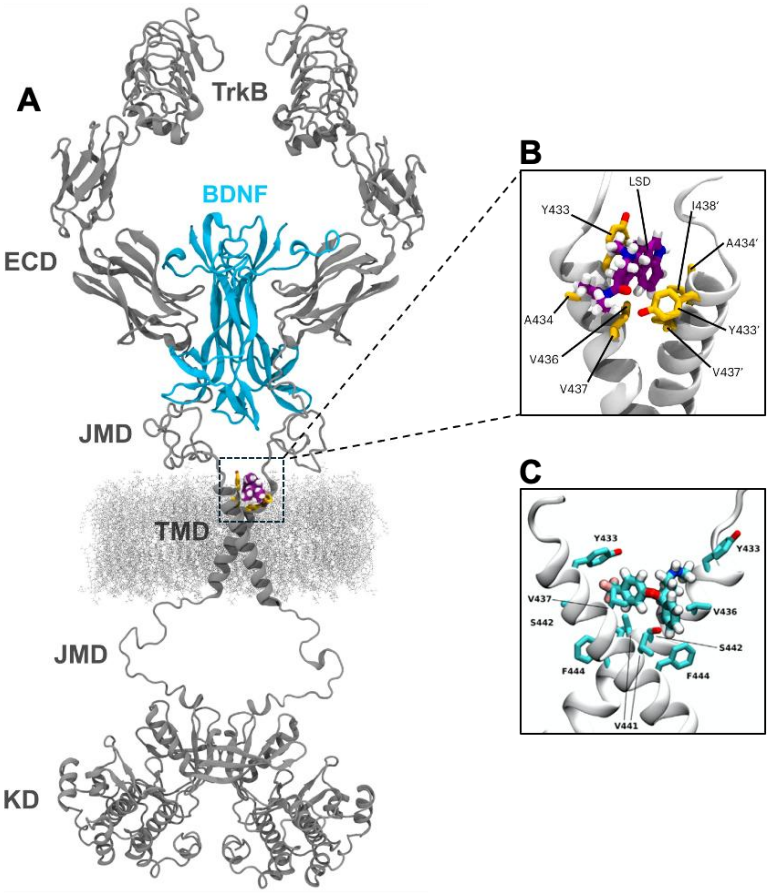

Figure 1. Structural organization of TrkB and proposed allosteric binding site.
(A) Schematic representation of TrkB receptor structure showing extracellular domain (ECD), juxtamembrane domain (JMD), transmembrane domain (TMD), and intracellular kinase domain (KD), BDNF bound within the ECD, and putative allosteric binding pocket for antidepressants and psychedelics within the TMD. **(B)** Representative structural model of lysergic acid diethylamine (LSD) bound within the allosteric binding pocket. **(C)** Representative structural model of fluoxetine bound within the allosteric binding pocket.
Figure adapted and combined with additional annotations and layout adjustments from Casarotto et al., 2021; Enkavi et al., 2024; Moliner et al., 2023. All source material is licenced under Creative Commons Attribution 4.0 (CC BY 4.0).

TrkB maturation from the immature protein persisting within endoplasmic reticulum (ER) to fully processed glycoprotein receptor located on the cell surface binding to BDNF is extensively dependent on N-glycosylation (Andreska et al., 2020; Haniu et al., 1995; Liu et al., 2014). This post-translational modification process is described in more detail in Figure

2. In addition to immaturely glycosylated forms, truncated isoforms are widely expressed in the CNS, particularly TrkB.T1 (Tessarollo & Yanpallewar, 2022). Truncated receptors lack the KD, thus being smaller proteins with similar molecular weight to immaturely glycosylated TrkB. Full-length mature TrkB is typically observed at 140–145 kDa, whereas immaturely glycosylated and truncated receptors have similar molecular weight, around 105 kDa and 95 kDa respectively (Haapasalo et al., 2002; Liu et al., 2014; Rantamäki et al., 2011).

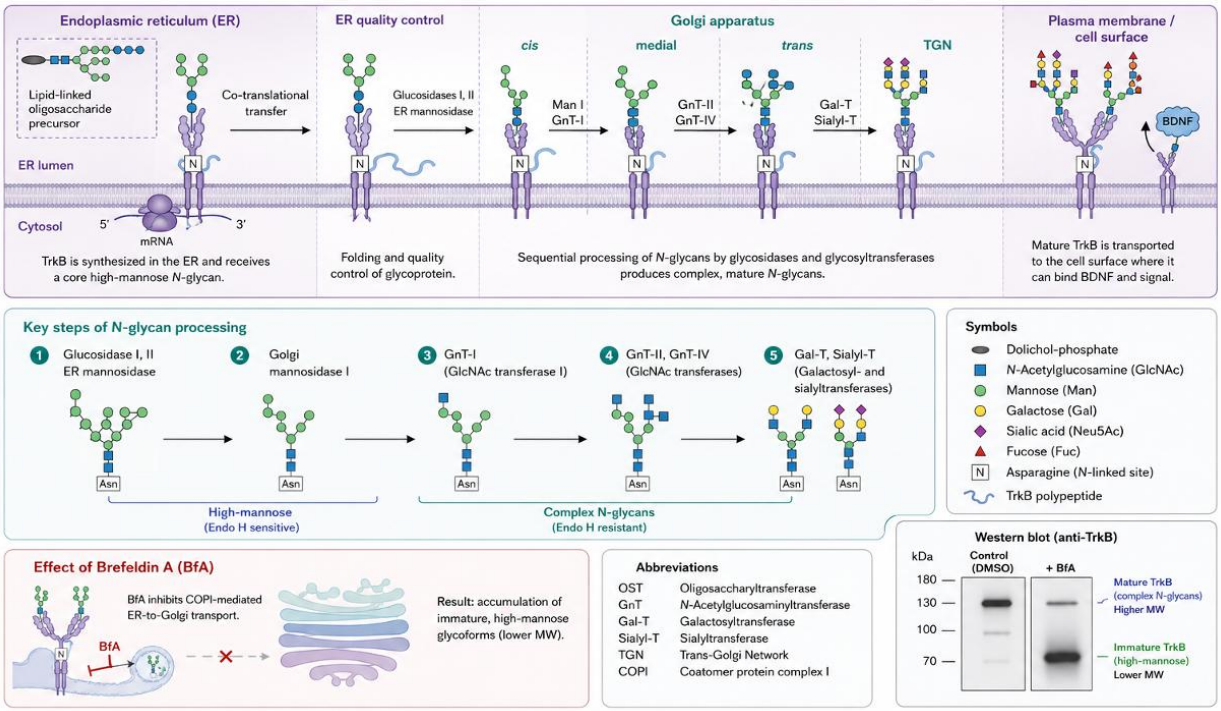

Figure 2. N-glycosylation, maturation and intracellular trafficking of TrkB in the secretory pathway, and the effect of brefeldin A treatment.
TrkB is synthesized in the endoplasmic reticulum (ER) and modified with high-mannose N-glycans, generating immaturely glycosylated TrkB. During ER quality control and subsequent trafficking through the cis-, medial-, and trans-Golgi compartments, the glycans are sequentially processed to produce mature glycoproteins. Maturely glycosylated TrkB is then transported to the plasma membrane where it can bind BDNF and initiate signaling. Brefeldin A (BfA) inhibits ER-to-Golgi transport, preventing glycan maturation and leading to accumulation of immature high-mannose glycoforms with lower molecular weight.
Figure generated using AI-assisted visualization and manually edited by the author, adapted from Bosshart et al., 1991; Haniu et al., 1995; Moremen et al., 2012; Stanley, 2011.

BDNF promotes TrkB activation through receptor dimerization leading to tyrosine autophosphorylation, thus initiating multiple intracellular signaling cascades, including the mitogen-activated protein kinase (MAPK), phosphoinositide 3-kinase (PI3K)-Akt, and phospholipase C-γ (PLC-γ) pathways (Chao, 2003; Coyle & Duman, 2003; Huang & Reichardt, 2003; Park & Poo, 2013). These pathways regulate gene expression, synaptic function, and neuronal connectivity, and are closely associated with mechanisms underlying long-term potentiation (LTP) and long-term depression (LTD), which are essential for

learning and memory. Importantly, BDNF expression and TrkB activation are tightly regulated by neuronal activity, allowing synaptic signaling to be translated into long-lasting structural and functional changes in neural circuits (Kuczewski et al., 2009; McAllister et al., 1999; Schinder & Poo, 2000; Thoenen, 1995; Zhao et al., 2009).

As impaired plasticity, disruptions in BDNF/TrkB signaling have been consistently associated with depression. Both clinical and preclinical studies have reported reduced BDNF expression and impaired TrkB signaling, particularly in brain regions involved in mood regulation such as the hippocampus and prefrontal cortex (Autry & Monteggia, 2012; Mitre et al., 2017). Chronic stress has been shown to decrease BDNF levels and impair synaptic plasticity, contributing to structural changes such as dendritic atrophy and reduced synaptic connectivity (Duman et al., 2016; Pittenger & Duman, 2008). These findings support the idea that dysregulation of neurotrophic signaling is not merely a consequence of depression but may play a causal role in its development.

Conversely, antidepressant treatments have been shown to enhance BDNF expression and activate TrkB signaling, thereby promoting synaptic plasticity and neuronal resilience (Castrén & Antila, 2017; Kraus et al., 2017; Nibuya et al., 1995; Rantamaki et al.; Rantamäki et al., 2011; Saarelainen et al., 2003). These effects are thought to underlie the ability of antidepressants to reverse stress-induced structural and functional deficits in neural circuits. Rather than acting solely through modulation of monoamine levels, antidepressants may exert their therapeutic effects by facilitating neuroplastic changes that restore adaptive network function over time.

Taken together, these findings highlight the central role of BDNF/TrkB signaling in linking neuronal activity, synaptic plasticity, and mood regulation. As such, this pathway represents a key molecular mechanism underlying both the pathophysiology of depression and the therapeutic effects of antidepressant treatments.

1.5 TrkB as a mediator and target of antidepressant action

Recent advances have significantly refined the understanding of antidepressant mechanisms, placing TrkB at the center of their therapeutic effects. While earlier models emphasized indirect activation of BDNF–TrkB signaling through increased monoaminergic neurotransmission, accumulating evidence suggests that antidepressants may also act more directly at the receptor level (Castrén & Antila, 2017; Kraus et al., 2017).

Several pharmacologically diverse antidepressants, including SSRIs like fluoxetine and rapid-acting agents such as ketamine, have been shown to directly interact with TrkB. These compounds bind to the TMD of the receptor and act as positive allosteric modulators, enhancing the responsiveness of TrkB to endogenous BDNF rather than directly activating the receptor in the absence of ligand (Casarotto et al., 2021). This mode of action provides a mechanistic explanation for how structurally and pharmacologically distinct antidepressants may converge on a common neuroplasticity-related pathway. Curiously, earlier studies have demonstrated rapid antidepressant-induced activation of TrkB signaling in also immaturely glycosylated receptor populations (Rantamäki et al., 2011; Saarelainen et al., 2003) suggesting that antidepressant effects on TrkB may involve multiple receptor pools differing in maturation state and cellular localization.

Importantly, the functional relevance of this interaction has been demonstrated in experimental models. Disruption of the TrkB TMD binding site, for example through point mutations, has been shown to abolish both the plasticity-promoting and behavioral effects of antidepressant treatments (Casarotto et al., 2021). Particular interest has focused on tyrosine 433 (Y433) corresponding to tyrosine 434 (Y434) in humans, which appears critical for antidepressant-TrkB interactions. These findings strongly support the idea that direct modulation of TrkB is not merely a biochemical observation but a critical component of antidepressant efficacy.

Within this framework, antidepressants can be understood as facilitators of neuroplasticity rather than simple modulators of neurotransmitter levels. By enhancing BDNF–TrkB signaling, these drugs promote synaptic remodeling, neuronal survival, and the reorganization of neural circuits that underlie mood regulation. This perspective aligns with the neuroplasticity hypothesis of depression, which emphasizes impaired adaptive capacity as a central feature of the disorder (Castrén, 2005; Castrén & Antila, 2017).

This model also provides a plausible explanation for the delayed onset of antidepressant effects. Although pharmacological interactions with monoamine systems occur rapidly, the therapeutic effects of antidepressants likely depend on the gradual induction of TrkB-mediated plastic changes and their integration into functional neural networks. These processes require time to develop, which may account for the delay between drug administration and clinical improvement (Duman & Monteggia, 2006; Kraus et al., 2017).

Taken together, these findings support a model in which TrkB acts as a central mediator of antidepressant action, linking pharmacological intervention to neuroplastic processes that enable recovery from depression. This has important implications for the development of novel treatments, as targeting TrkB signaling directly may offer a more effective strategy than approaches focused solely on monoaminergic neurotransmission.

1.6 Rapid-acting antidepressants and psychedelics

The limitations of conventional antidepressants, particularly their delayed onset of action and modest efficacy, have driven increasing interest in treatments that can produce more rapid and robust therapeutic effects. One of the most important developments in this area has been the discovery of the rapid antidepressant effects of ketamine, an N-methyl-D-aspartate (NMDA) receptor antagonist. Unlike traditional antidepressants, ketamine can induce significant symptom relief within hours, even in treatment-resistant patients, thereby challenging the monoamine-centered framework of depression (Berman et al., 2000; Duman et al., 2016).

The antidepressant effects of ketamine have been strongly linked to its ability to rapidly enhance synaptic plasticity. Preclinical studies have shown that ketamine increases synaptogenesis, dendritic spine density, and functional connectivity in brain regions implicated in mood regulation, particularly the prefrontal cortex (Cannarozzo et al., 2023; Castanheira et al., 2025; Ly et al., 2021; Ma et al., 2017). These findings further support the neuroplasticity hypothesis of depression, suggesting that rapid induction of synaptic remodeling may underlie fast-acting antidepressant effects.

In parallel with ketamine research, classical serotonergic psychedelics such as lysergic acid diethylamide (LSD) and psilocybin have gained increasing attention as potential rapid-acting antidepressants. Clinical studies have demonstrated that these compounds can produce rapid and, in some cases, long-lasting reductions in depressive symptoms, even after a limited number of administrations (Carhart-Harris & Goodwin, 2017; Vargas et al., 2021). In addition to their clinical effects, psychedelics have been shown in preclinical models to promote structural plasticity, including increased dendritic branching, spine formation, and synaptic density, leading to the concept of psychoplastogens (Ly et al., 2018).

Traditionally, the effects of classical psychedelics have been attributed primarily to activation of the serotonin 5-HT_{2A} receptor, which is closely associated with their hallucinogenic and subjective effects. However, emerging evidence suggests that their plasticity-promoting and antidepressant-like effects may not be fully dependent on this pathway. In particular, studies have shown that some aspects of psychedelic-induced plasticity can persist even when 5-HT2A signaling is pharmacologically blocked, indicating the involvement of additional mechanisms (Ly et al., 2018).

One such mechanism involves BDNF–TrkB signaling. Recent findings suggest that psychedelics can also directly interact with TrkB and enhance BDNF-mediated signaling. LSD and psilocin have been shown to bind to the TMD of TrkB and act as positive allosteric modulators analogous to conventional antidepressants (Moliner et al., 2023). Notably, these compounds appear to interact with TrkB with profoundly higher affinity, which may contribute to their more rapid and pronounced effects on synaptic plasticity.

These observations raise the possibility that both conventional antidepressants and psychedelics may converge on a shared mechanism involving TrkB-mediated neuroplasticity, despite having distinct primary pharmacological targets. At the same time, the relative contribution of TrkB signaling and classical serotonergic pathways to the therapeutic effects of psychedelics remains an open question. Further research is therefore needed to clarify how these mechanisms interact and to what extent TrkB modulation alone is sufficient to produce antidepressant effects.

Taken together, the study of rapid-acting antidepressants and psychedelics supports a model in which modulation of neuroplasticity, particularly through BDNF–TrkB signaling, represents a central mechanism underlying both rapid and sustained antidepressant responses. This provides a strong rationale for further investigation of TrkB as a therapeutic target and for the development of novel compounds that can selectively enhance plasticity without undesirable side effects.

Figure 3 provides an overview of BDNF–TrkB signaling in the healthy and depressed brain and the proposed modulation of TrkB by antidepressants and psychedelics.

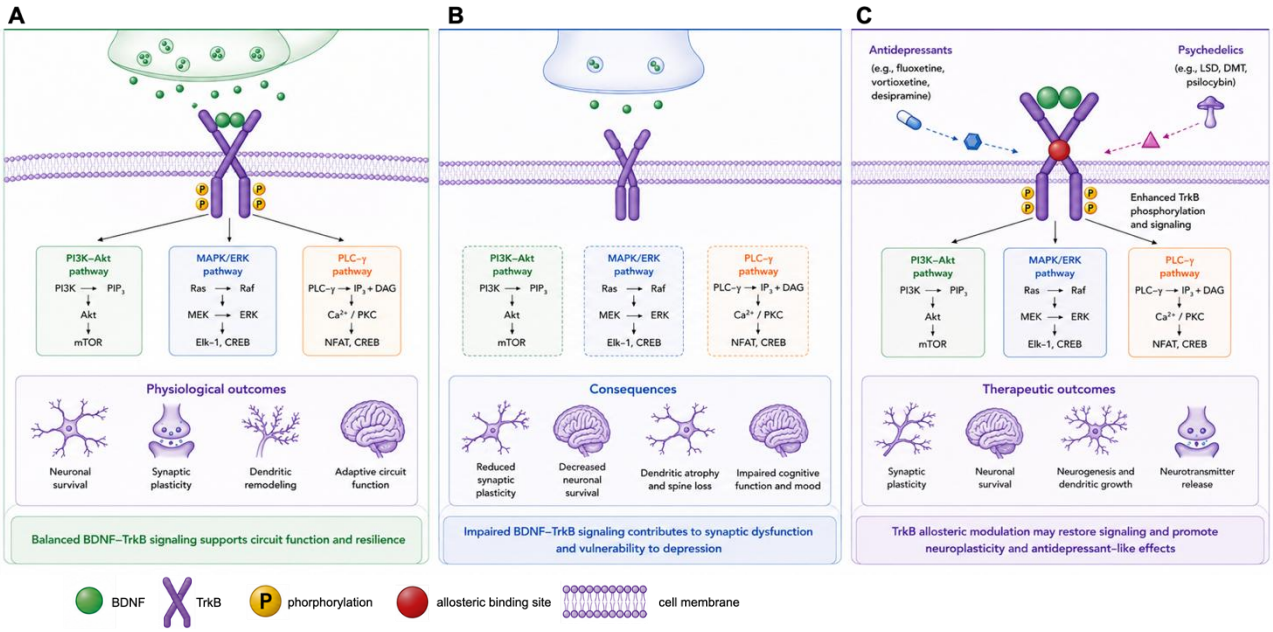

Figure 3. BDNF–TrkB signaling in the healthy brain, depression, and modulation by antidepressants and psychedelics.
(A) In the healthy brain, binding of brain-derived neurotrophic factor (BDNF) to tropomyosin receptor kinase B (TrkB) promotes receptor dimerization and autophosphorylation, leading to activation of downstream signaling pathways including phosphoinositide 3-kinase (PI3K)–Akt, mitogen-activated protein kinase/extracellular signal-regulated kinase (MAPK/ERK), phospholipase C-γ (PLC-γ). These signaling pathways support neuronal survival, synaptic plasticity, dendritic remodeling, and adaptive neural circuit function. **(B)** In depression, reduced BDNF availability and impaired TrkB signaling are associated with decreased synaptic plasticity, impaired neuronal resilience, and maladaptive neural circuit function. **(C)** Antidepressants and classical psychedelics have been shown to bind allosterically to TrkB, enhancing BDNF-mediated signaling and promoting neuroplasticity-related responses.
Figure created using AI-assisted visualization and manually refined by the author based on information synthesized from the cited literature.

1.7 Methods to study ligand–TrkB interactions

Studying ligand–TrkB interactions requires techniques capable of detecting relatively weak and potentially context-dependent binding events in membrane proteins. Various biophysical binding assays, such as surface plasmon resonance (SPR), microscale thermophoresis (MST) competition binding or receptor dimerization assays, have been used to assess receptor–ligand interactions and thus, have contributed substantially to the current understanding of antidepressant and psychedelic binding to TrkB (Casarotto et al., 2021; Hunter et al., 2025; Jerabek-Willemsen et al., 2014; López-Méndez et al., 2021; Moliner et al., 2023).

For high- throughput ligand binding studies, spectral shift (SpS) and temperature-related intensity change (TRIC) are techniques enabling highly sensitive detection of binding-induced fluorescence changes (Langer et al., 2022). These techniques are compatible with

native biological samples (e.g., tissue and cell extracts), are performed in biological conditions (buffers, temperature), and non-immobilized conditions. These features make it an attractive methodology for novel ligand discovery.

However, studying TrkB binding remains technically challenging. In vitro models commonly used for receptor studies include HEK293T cells, stably expressing cell lines, or cancer cell lines (PC12, N2A), each with different advantages and limitations in terms of receptor expression, membrane environment, and physiological relevance (Antila et al., 2014). For instance, overexpression systems may facilitate detection but can also introduce artifacts related to receptor abundance leading to ligand independent, spontaneous receptor dimerization and activation, trafficking, and glycosylation state, complicating interpretation of both binding and downstream signaling results (Biojone et al., 2024; Vesa et al., 2000).

TrkB glycosylation state is particularly relevant since the two forms differ greatly in receptor maturation, membrane localization and ligand accessibility. These aspects are particularly relevant in lysate-based binding assays, where heterogeneous receptor populations containing both mature and immature glycosylation states may coexist simultaneously and influence receptor accessibility, conformational stability, and assay performance. In this context, brefeldin A (BfA), an inhibitor of ER-to-Golgi transport, can be used experimentally to disrupt TrkB maturation process and enrich immature glycosylated receptor forms, thereby helping to assess whether distinct molecular weight bands represent maturation states of TrkB (Bosshart et al., 1991; Haniu et al., 1995; Moremen et al., 2012; Zhao et al., 2009).

These technical considerations are especially important when evaluating weak or allosteric binding events, where assay buffer composition/pH, labeling strategies, receptor glycosylation, and expression model can substantially influence the observed results. Accordingly, careful assay validation is necessary before mechanistic conclusions can be drawn from ligand–TrkB interaction studies.

1.8 Gaps in knowledge and rationale of the present study

Although the role of TrkB in antidepressant action is now strongly supported, several important questions remain unresolved. First, the importance of direct versus potential indirect TrkB activation remains under active debate. It is still not fully clear to what extent the antidepressant and psychedelic effects on TrkB depend on endogenous BDNF, how

much is explained by allosteric modulation, and whether canonical ligand-dependent activation and non-canonical drug-induced modulation should be viewed as distinct or overlapping mechanisms (Biojone et al., 2024; Brunello et al., 2024; Casarotto et al., 2021; Ly et al., 2021).

Second, technical and biological variability in receptor expression systems may substantially affect conclusions. Transfection efficiency, receptor overexpression, membrane trafficking, and glycosylation state may all alter receptor conformation and apparent ligand accessibility, raising the possibility that some experimental systems do not fully reflect physiologically relevant TrkB behavior. This is particularly important for membrane receptors such as TrkB, where maturation status and membrane context may strongly influence function.

Third, available binding studies remain relatively limited, especially in cell lysate-based or more native-like systems. While purified-protein approaches have provided important mechanistic insight, they may not fully capture the influence of membrane composition, post-translational modifications, or associated proteins. Conversely, crude cellular systems may preserve more native conditions but introduce uncertainty in receptor quantification and biochemical heterogeneity.

Collectively, these unresolved biological and methodological questions provide the rationale for the present study, which aimed not only to investigate ligand interactions with TrkB but also to establish a sufficiently robust experimental framework for reliable interpretation of lysate-based binding measurements.

1.9 Aim of the study

The original aim of this study was to investigate ligand interactions with the neurotrophic receptor TrkB using the newly introduced Dianthus binding affinity screening platform (Nanotemper, Germany) and to evaluate whether classical psychedelics and other selected compounds could be analyzed using this approach. The broader rationale of this work was to explore whether psychedelics may interact with TrkB within concentration ranges potentially relevant to antidepressant effects independent of 5-HT_{2A} mediated hallucinogenic activity.

As the project progressed, it became evident that reliable binding analysis required prior characterization, development and optimization of the assay system. Therefore, the study objectives evolved to include:

1. Establishment and optimization of Dianthus-based binding measurements for TrkB-containing cell lysates.
2. Estimation of TrkB concentrations in experimental samples using Western blotting and enzyme-linked immunosorbent assay (ELISA).
3. Characterization of TrkB molecular heterogeneity and glycosylation state.
4. Preliminary evaluation of selected ligands, including LSD.
5. Identification of technical and biological factors influencing ligand detection in lysate-based systems.

Taken together, the study aimed to generate a practical framework for future high-quality TrkB binding studies while providing initial observations on selected candidate ligands.

2 Materials and Methods

Key reagents and antibodies used in this study are summarized in Tables 1 and 2.

Table 1. Key resources

Reagent or resource	Source	Identifier
HEK293FT	ThermoFisher Scientific	RRID:CVCL_6911
DMEM	ThermoFisher Scientific	Cat#21969035
Fetal bovine serum	ThermoFisher Scientific	Cat#10500064
Opti-MEM™	ThermoFisher Scientific	Cat#31985047
L-Glutamine	ThermoFisher Scientific	Cat#25030024
Penicillin-Streptomycin	ThermoFisher Scientific	Cat#15140122
FuGENE® 6 Transfection Reagent	Promega	Cat#E2691
cOmplete™ Protease Inhibitor Cocktail	Merck	Cat#4693132001
Sodium Orthovanadate (Na3VO4)	Merck	Cat#450243
Recombinant Human TrkB Fc Chimera Protein, CF	R&D Systems	Cat#688-TK
Human Total TrkB DuoSet™ IC ELISA	R&D Systems	Cat#DYC397-5
DuoSet ELISA Ancillary Reagent Kit 2	R&D Systems	Cat#DY008B
Sample Diluent Concentrate 2 (2X)	R&D Systems	Cat#DYC002
Thiazolyl Blue Tetrazolium Bromide (MTT)	Sigma-Aldrich	Cat#M2128
His-Tag Labeling Kit RED-tris-NTA 2nd Gen	NanoTemper	Cat#MO-L018
ECL Plus	ThermoFisher Scientific	Cat#32132

Table 2. Antibodies used for Western blotting

Antibody	Host	Application	Dilution	Source	Identifier
anti-TrkB	Goat	Primary	1:1000	R&D Systems	Cat#AF1494
anti-GAPDH	Mouse	Primary	1:2000	Abcam	Cat#ab8245
anti-turboGFP	Mouse	Primary	1:100	Origene	Cat#TA150041
anti-rabbit HRP	Goat	Secondary	1:5000	Dako	Cat#170-5046
anti-mouse HRP	Goat	Secondary	1:5000	Dako	Cat#170-6516

2.1 Cell Culture and Maintenance

HEK293T cells were cultured in Dulbecco's Modified Eagle Medium (DMEM) supplemented with 10% fetal bovine serum, D-glucose (4.5 g/L), penicillin (50 U/mL)/streptomycin (50 µg/mL), and L-glutamine (2 mM). Cells were maintained at 37 °C in a humidified atmosphere containing 5% CO_2 and split at 70–80% confluence.

Cells were washed with prewarmed 1X phosphate-buffered saline (PBS), detached with 2 mL trypsin-EDTA (0.25%) and incubated at +37 °C, 5% CO_2 for 2-5 min. Cells in trypsin were collected to falcon tube, the plate was washed with 10 mL supplemented DMEM to collect leftover cells, and cell suspension was centrifuged (3 min, 100 rcf). Medium supernatant was aspirated, and cell pellet was resuspended in DMEM by gentle pipetting. Cell suspension was then transferred to a new plate containing prewarmed supplemented DMEM at a 1:10 to 1:20 splitting ratio.

2.2 Transfection Protocol

At 60–80% confluence, cells were transiently transfected to overexpress TrkB (full-length TrkB.wt, unless otherwise mentioned) using FuGENE 6® as transfection agent with expression plasmid encoding TrkB either carrying a 6x Histidine repetition tag (His-tag) or with fluorescent fusion protein mCardinal for labelling. Plasmid was prepared to have a final concentration of 2 μg/mL in the plate and FuGENE® 6/DNA complex was prepared at a 3:1 ratio according to the manufacturer's instructions.

Briefly, FuGENE 6® was added to serum-free medium (Opti-MEM™) followed by DNA after 5 min incubation at room temperature (RT). FuGENE 6®/DNA mixture was incubated 15 min RT before introducing to cells. Cells were incubated for 24–48 h prior to downstream analyses.

2.3 Cell Lysis and Sample Preparation

Cells were placed on ice, washed with ice-cold 1X PBS, lysed in cold Nonidet P-40 (NP-40)-based lysis buffer (20 mM Tris–HCl, 137 mM NaCl, 10% glycerol, 50 mM NaF, and 1% NP-40) supplemented with phosphatase inhibitor and protease inhibitor cocktail, and detached using a cell scraper. Lysates were optionally sonicated prior to clarification by centrifugation (+4 °C, 15 min, 16 000 × g). Supernatants were collected and kept on ice for immediate use or stored at −80 °C for later analysis.

Two methods for mechanical lysis were also evaluated; 1) using a disposable pestle and 2) passing the lysate several times through a low gauge needle attached to a 1 mL syringe. PBS with Tween® 20 0.05% (PBS-T) supplemented with phosphatase inhibitor and protease inhibitor cocktail was used as a buffer.

2.4 Protein Quantification

2.4.1 Total Protein Concentration

To ensure equal protein loading for electrophoresis and to estimate lysate concentrations for downstream analyses, total protein concentrations were determined using Bio-Rad's *DC* protein assay according to microplate assay protocol from manufacturer's instruction manual.

Lysate dilutions of 1:5, 1:10 and 1:100 was used, and dilution series of bovine serum albumin (BSA) protein standards were prepared in the same buffer as lysates to obtain standard curve from 2 mg/mL to 0 mg/mL. The assay was run in 96-well microplates with duplicates of samples and standards. After incubation 15 min RT absorbance was measured at 750 nm using Varioskan Flash (Thermo Scientific) microplate reader.

2.4.2 Western Blotting

Lysates were mixed 1:1 with 2X Laemmli sample buffer and denatured for 5 min at +95 °C. To remove impurities from the gel wells, running buffer was pipetted in and out of the wells and a short blank electrophoresis run was performed before loading the samples.

Proteins were separated according to molecular weight by sodium dodecyl-sulfate polyacrylamide gel electrophoresis (SDS–PAGE) under reducing conditions. Approximately 10 µg of protein in Laemmli buffer was loaded per lane on a precast gradient gel, and a protein ladder was used as a molecular weight marker. Glyceraldehyde 3-phosphate dehydrogenase (GAPDH) was used as a loading control for lysate samples, while recombinant TrkB standards were included in selected blots to estimate the amount of TrkB present in the cell lysates. Empty wells were loaded with Laemmli buffer for negative control. Electrophoresis was run either 120 V RT or 200 V +4 °C for approximately 2 h.

Proteins were transferred to a polyvinylidene fluoride (PVDF) membrane using Tran-Blot Turbo Transfer System (Bio-Rad) (2.5 A, 25 V, 30 min). Subsequently, the membrane was briefly washed with tris-buffered saline with Tween® 20 0.05% (TBS-T) and blocked in 3% BSA in TBS-T for 1 h RT. The membrane was then cut and the TrkB and GAPDH portions were incubated with their respective primary antibodies overnight at +4 °C on a shaker. After three washes with TBS-T, the membranes were incubated with the corresponding horseradish peroxidase (HRP) -conjugated secondary antibodies for 1 h RT on a shaker.

After additional washes with TBS-T, protein bands were visualized using enhanced chemiluminescent substrate (ECL Plus) and imaged using a charge-coupled camera camera (G:BOX Chemi XX6, Syngene). Images were processed using Fiji (ImageJ, NIH, v.2.14.0/1.54f).

2.4.3 ELISA for TrkB Quantification

TrkB concentrations in cell lysates were also measured by a sandwich ELISA using the Human Total TrkB DuoSet™ IC ELISA kit combined with DuoSet™ ancillary products according to the manufacturer's instructions.

Five different batches of TrkB-His cell lysates (S1-S5) and one TrkB-GFP lysate batch (S6) were included in the assay. Samples were analyzed using both 1:10 and 1:100 dilutions to ensure measurements remained within the dynamic range of the assay. Reagent diluent concentrate 2 (2X) was used for dilutions, and it was prepared according to manufacturer's instructions to obtain 1% BSA in PBS. Human Total TrkB Standards were prepared in 2-fold dilution series ranging from 0 to 6 ng/mL. Optical density (OD) was measured at 450 nm with wavelength correction at 570 nm using Varioskan Flash microplate reader. Corrected OD values were calculated by subtracting the 570 nm reference OD from the 450 nm measurement.

The four-parameter logistic (4PL) regression model was used for standard curve fitting and concentration calculations due to poor fit of the linear model. Concentrations obtained from diluted samples were corrected using the corresponding dilution factors. Mean values, standard deviations and coefficients of variation were calculated from duplicate measurements.

2.5 Glycosylation experiments using Brefeldin A

First, the maximal duration of BfA treatment was examined using the manufacturer-recommended concentration (1:1000 dilution), maximal effect being maximal amount of immaturely glycosylated protein and maximal cell viability. Cells were treated with BfA for either approximately one or two days (22 h and 44 h). Untreated control wells (n=30) and BfA-treated wells (n=30) were included for both exposure durations.

Subsequently, the optimal BfA concentration was evaluated using 2-fold serial dilutions ranging from 1:1000 to 1:5000. In parallel, the effects of short versus previously determined

maximal treatment exposure and high versus low confluence were investigated. Each condition was initially analyzed with n=10, although final sample sizes varied slightly due to missing measurements.

Finally, the optimal sequence to perform BfA treatment and transfection was examined. Different treatment schedules were tested to determine whether BfA treatment should be performed before, after or concurrently with transfection. Experimental treatment schedules are summarized in Figure 4.

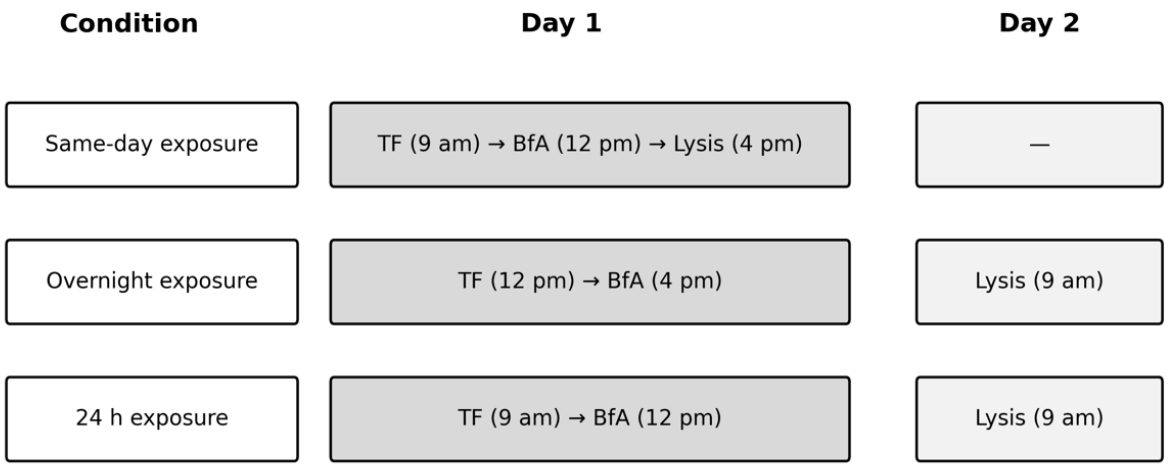

Figure 4. Experimental schedules for treatment sequence optimization

Schematic overview of transfection, brefeldin A treatment and lysis timing used to evaluate the effects of exposure duration on TrkB expression, glycosylation state, and cell viability. Same-day exposure samples were lysed on the same day, whereas overnight and 24 h exposure samples were lysed on the following morning. Abbreviations: TF = transfection, BfA = brefeldin A

HEK293T cells were transfected to express TrkB fused with GFP, enabling visualization of transfection efficiency by fluorescence microscopy. Cell morphology was additionally monitored under transmitted light to assess viability.

2.5.1 MTT assay

MTT (3-(4,5-dimethylthiazol-2-yl)-2,5-diphenyltetrazolium bromide) assay was used to assess cell viability.

Cells were distributed randomly into 96-well plates at approximately 5000 cells per well. The outermost wells were filled with distilled water (dH_2O) to reduce evaporation. At each time point, 5 µl of MTT solution (5 mg/mL in PBS) was added to each well and incubated for 2 h at +37 °C. Following incubation, 100 µL of MTT lysis buffer (10% SDS, 10mM

HCl in dH_2O) was added to each well and plates were incubated overnight at +37 °C. Absorbance was measured at 540 nm using Varioskan Flash microplate reader.

2.6 Dianthus Binding Assays

Ligand-binding measurements were performed using the Dianthus platform.

HEK293T cell lysates expressing His-tagged TrkB were used. TrkB was fluorescently labelled using Nanotemper's own RED-tris-NTA 2nd Generation His-tag labeling kit according to the manufacturer's instructions. Labeling was performed directly in lysates without prior protein purification. Excess unbound dye was not removed, as permitted by the labeling protocol. Following labeling, samples were diluted into PBS-T, unless otherwise indicated. In selected optimization experiments, TrkB with mCardinal and lysates prepared in NP-40-based lysis buffer or mechanically disrupted lysates in PBS-compatible buffer were also evaluated.

Ligands were mixed 1:1 with labeled TrkB samples to obtain final assay concentrations. Binding checks were run with positive control in triplicates, and binding affinities were run in duplicates. 16 point two-fold dilution series were used for binding affinity testing. The final assay volume was 20 µL per well in NanoTemper 384-well plates.

Samples were mixed by gently pipetting and briefly centrifuged prior to measurement to remove air bubbles and ensure uniform well filling. Measurements were performed using the Dianthus instrument according to manufacturer-recommended settings.

3 Results

3.1 Detection and Quantification of TrkB Expression in HEK293T Cell Lysates

To determine whether the cells successfully expressed TrkB and to estimate receptor concentrations for downstream binding experiments, HEK293T cell lysates were analyzed by both Western blotting and ELISA.

3.1.1 Western Blot Analysis

Western blot analysis was conducted using lysates from HEK293T cells transfected to express either full-length TrkB or Y433F mutation. Recombinant human TrkB Fc chimera protein (RcTrkB) was included as a reference standard to enable approximate comparison of signal density.

Prominent immunoreactive bands corresponding to TrkB.wt was detected at approximately 145 kDa in all transfected samples (Figure 5A,B). The molecular weights observed were consistent with expectations, with fusion proteins appearing as larger molecules compared to the His-tagged proteins. In addition to the main band, several lower molecular weight bands were consistently detected across lysates. These bands could represent alternative receptor forms, such as immaturely glycosylated species, partially processed products, or truncated isoforms.

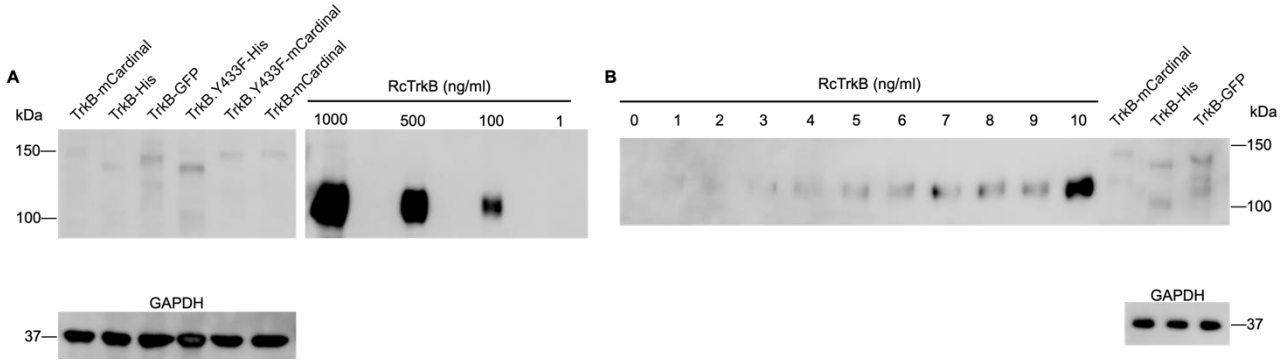

Figure 5. Estimation of TrkB concentration in HEK293T cell lysates using Western blotting. Representative Western blot images used for estimation of TrkB abundance in lysates expressing TrkB constructs. Recombinant Human TrkB Fc Chimera Protein (RcTrkB) was used as a reference standard for approximate protein quantification. Multiple TrkB-immunoreactive bands were observed, consistent with heterogeneous receptor populations and different forms of TrkB. GAPDH was used as a loading control where applicable. **(A)** Preliminary blot during initial optimization. **(B)** Blot from later optimization stages showing improved TrkB detection and comparison with recombinant TrkB standard.

Initial blots using a broad concentration range of RcTrkB were sufficient to confirm expression but were suboptimal for quantitative comparison (Figure 5A). Subsequent blots using lower RcTrkB concentrations improved comparability between lysates and RcTrkB allowing a rough estimate that TrkB abundance in lysates was within the low ng/µL total protein range (Figure 5B). However, precise densitometric analysis could not be performed.

GAPDH was used as a loading control for lysate samples and demonstrated consistent and comparable loading between lanes. As expected, no GAPDH signal was detected in lanes containing RcTrkB.

Overall, Western blotting confirmed robust TrkB expression in transfected HEK293T cells while also indicating the presence of multiple receptor forms in the lysates.

3.1.2 ELISA Quantification

To obtain a more quantitative estimate of TrkB concentration, HEK293T lysates were further analyzed using a commercial ELISA kit specific for total TrkB. The 4PL regression model provided improved fitting of the standard curve compared with a linear model and was therefore used for concentration interpolation. (Figure 6A).

The dilution-corrected TrkB concentrations ranged approximately from 15 ng/mL to 61 ng/mL depending on the lysate preparation (Figure 6B). Samples S1–S5 represent independent lysate preparations expressing the same His-tagged TrkB construct, whereas S6 represents a lysate expressing the TrkB-mCardinal construct. Highly diluted (1:100) samples produced inconsistent absorbance values and disproportionate variability between duplicates indicating poor sample quality, thus only 10-fold diluted samples were included in the final graphical presentation and concentration comparison.

Some samples showed relatively low variability between duplicate measurements, whereas others demonstrated substantially higher variation, reflected by elevated coefficients of variation. In particular, samples S2-S5 with absorbance values approaching the upper region of the standard curve exhibited increased variability, which may have reduced interpolation accuracy.

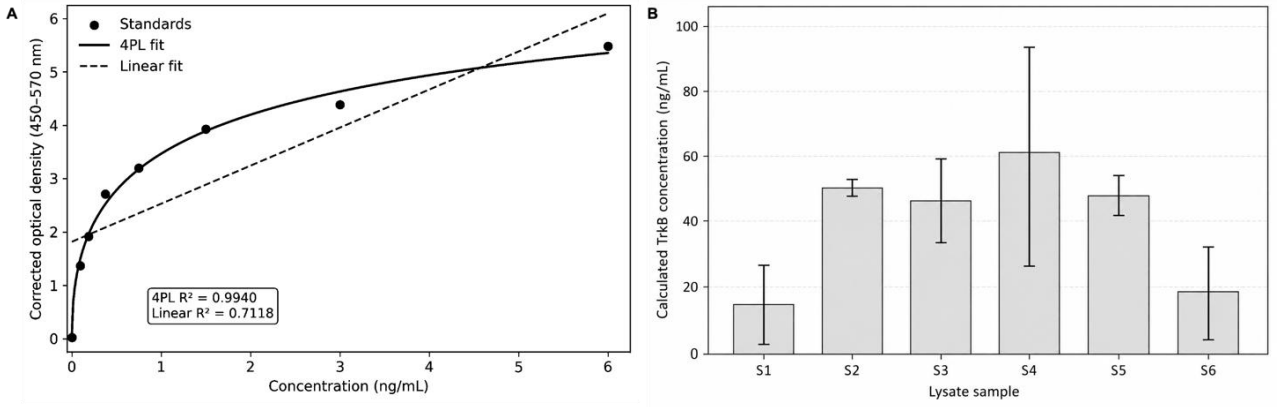

Figure 6. Estimation of TrkB concentration in HEK293T cell lysates using ELISA.
(A) Representative standard curve generated using the commercial Human Total TrkB DuoSet™ IC ELISA kit and fitted with 4PL regression model. **(B)** Calculated TrkB concentrations in independent, 10-fold diluted lysates. Samples S1–S5 represent independent lysate preparations expressing the same His-tagged TrkB construct. S6 represents lysate preparation expressing TrkB-mCardinal. Concentrations were calculated from interpolated absorbance values using the 4PL standard curve. Bars represent mean ± SD of duplicate measurements. Highly diluted samples showing inconsistent interpolation behavior were excluded from the final graphical presentation.

Despite variability between some measurements, the ELISA-derived TrkB concentrations aligned reasonably well with the approximate TrkB abundance obtained observed by Western blotting. Taken together, these results from both analyses confirmed that HEK293T lysates contained sufficient TrkB expression and provided sufficiently robust estimates of TrkB concentrations for subsequent ligand-binding studies.

3.2 Glycosylation Status of TrkB

To further characterize the multiple TrkB bands observed in Western blotting, additional experiments were performed to assess whether these bands reflected differences in receptor maturation and glycosylation state. As TrkB is a membrane receptor that undergoes post-translational maturation in the ER and Golgi apparatus, incomplete glycosylation may shift its molecular weight, trafficking, and ligand-binding properties.

BfA was used to disrupt normal post-translational processing and enrich immaturely glycosylated receptor forms in the lysates. Given the cytotoxic nature of BfA, treatment conditions were optimized to maximize the accumulation of immaturely glycosylated TrkB while maintaining acceptable cell viability. Optimization experiments included evaluation of treatment duration, BfA concentration, cell confluence, and treatment sequence relative to transfection.

3.2.1 Effect of exposure time on cell viability

To determine a suitable maximum exposure time for BfA treatment, cell viability was assessed by MTT assay following 22 h and 44 h exposure at a 1:1000 dilution. After 22 h, viability remained at approximately 77% relative to untreated controls, whereas 44 h exposure reduced viability to approximately 45% (Figure 7A). Based on these findings, the maximum BfA exposure was set to 24 h to enhance the disruption of receptor maturation without compromising sample quality.

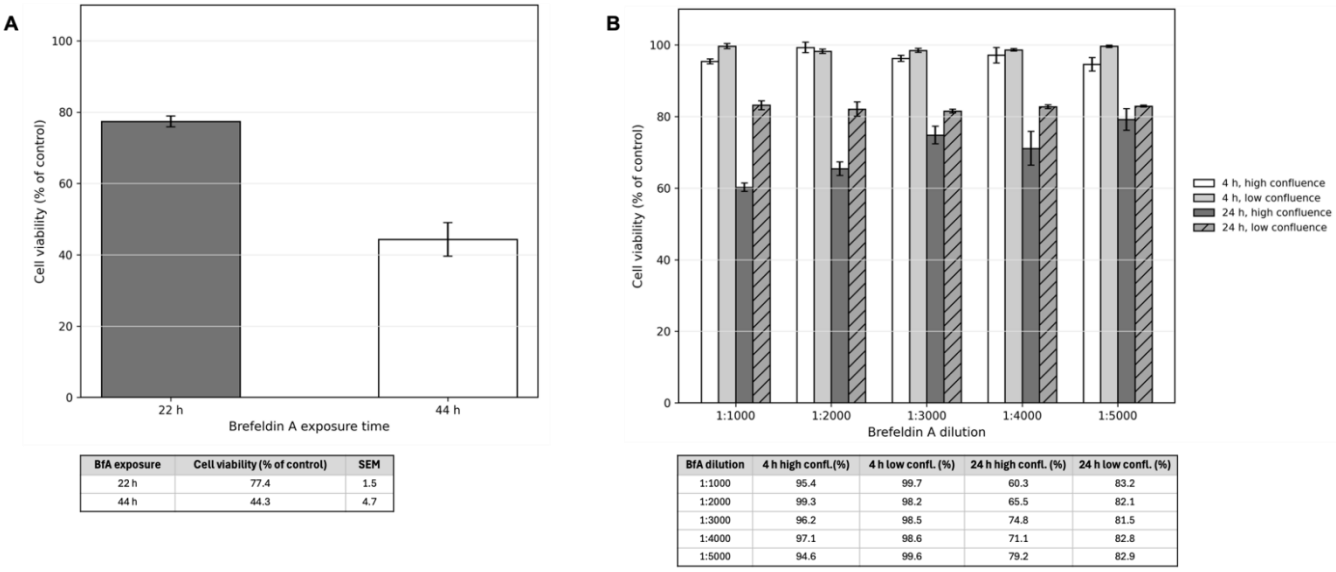

BfA exposure	Cell viability (% of control)	SEM
22 h	77.4	1.5
44 h	44.3	4.7

BfA dilution	4 h high confl.(%)	4 h low confl. (%)	24 h high confl. (%)	24 h low confl. (%)
1:1000	95.4	99.7	60.3	83.2
1:2000	99.3	98.2	65.5	82.1
1:3000	96.2	98.5	74.8	81.5
1:4000	97.1	98.6	71.1	82.8
1:5000	94.6	99.6	79.2	82.9

Figure 7. Effect of Brefeldin A exposure duration on HEK293T cell viability.
(A) HEK293T cells were treated with BfA at a final dilution of 1:1000 for either 22 h or 44 h. Prolonged exposure greatly reduced cell viability compared with shorter exposure conditions, supporting the maximum treatment duration to approximately 24 h in subsequent experiments.
(B) HEK293T cells were exposed to serial dilutions of BfA (1:1000–1:5000) under conditions of high or low confluence and short (4 h) or maximum (24 h) exposure duration. Viability varied depending on both treatment duration and cell density, indicating that optimization of experimental conditions was necessary to balance accumulation of immature glycosylated TrkB with acceptable cell viability.

3.2.2 Effect of BfA concentration, short exposure and cell confluence on cell viability

The optimal concentration of BfA was determined starting from the manufacturer's recommendation 1:1000 dilution, with subsequent 2-fold dilutions down to 1:5000. Concurrently, the effects of short versus long treatment exposure time and high versus low cell confluence were examined (Figure 7B).

Cell viability reduced in concentration-dependent manner only in high-confluence cultures with 24 h exposure, viability ranging from approximately 60% to 79%. Dilution of BfA did

not markedly improve viability relative to the manufacturer-recommended concentration. Therefore, the recommended 1:1000 dilution was retained for subsequent experiments.

4 h exposure had minimal effect on viability under both high- and low-confluence conditions, with values generally remaining above 95% of controls. In contrast, 24 h exposure reduced viability, notably in high-confluence cultures as mentioned. Low-confluence cultures were less affected, maintaining approximately 81–83% viability after 24 h treatment.

3.2.3 Treatment sequence effect

The optimal sequence of transfection and BfA treatment was investigated because both procedures impose substantial cellular stress and may influence cell viability, transfection efficiency, and TrkB processing. Ideally, BfA treatment would precede transfection in order to maximize accumulation of immaturely glycosylated TrkB. However, when BfA treatment was performed before or concurrently with transfection, cell viability decreased markedly and transfection efficiency remained poor, as indicated by reduced GFP fluorescence and altered cell morphology (Figure 8A,B).

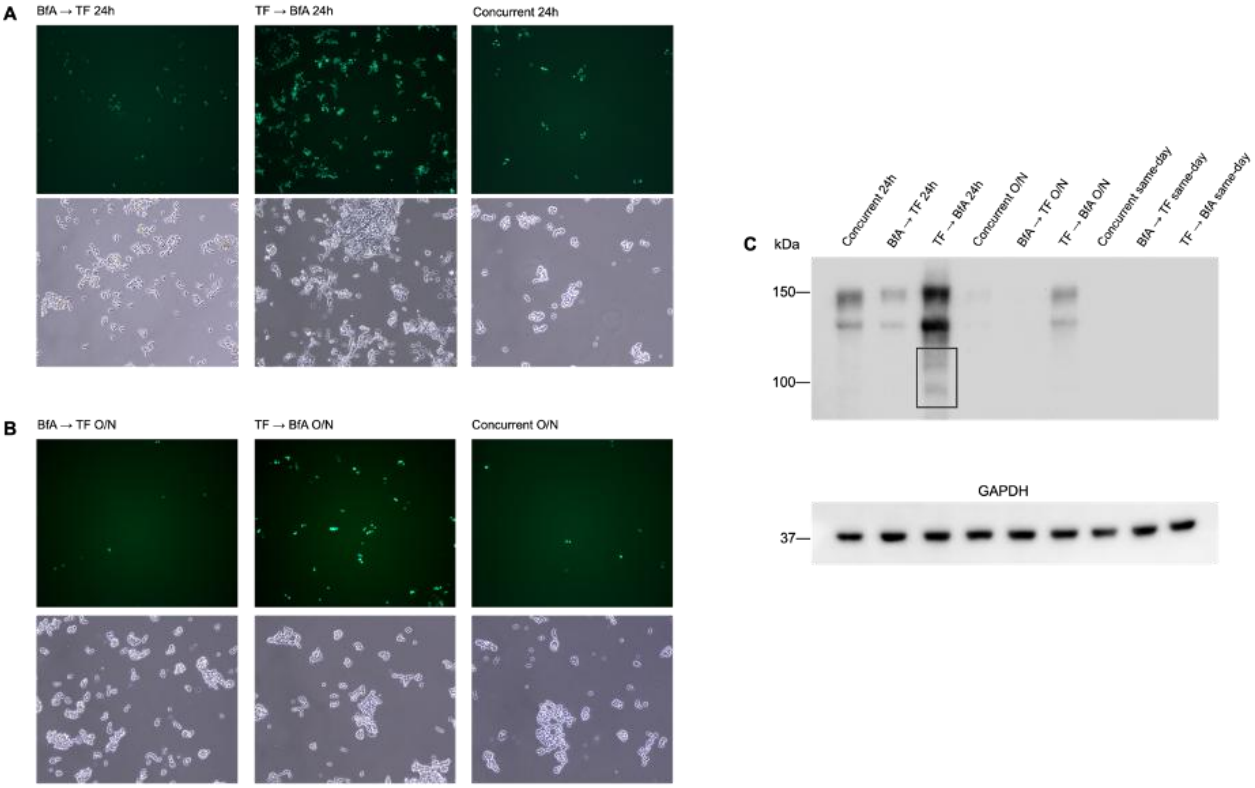

Figure 8. Effects of Brefeldin A treatment sequence on TrkB-GFP expression, cell morphology, and TrkB banding pattern.
(A) Fluorescence (upper panel) and transmitted-light (lower panel) microscopy images of HEK293T cells expressing TrkB-GFP following different BfA treatment schedules with 24 h exposure.

(B) Fluorescence (upper panel) and transmitted-light (lower panel) microscopy images of HEK293T cells expressing TrkB-GFP following different BfA treatment after overnight BfA exposure.
(C) Western blot analysis of TrkB expression under the tested treatment conditions. The condition in which BfA treatment was applied after transfection with 24 h exposure produced the most prominent lower molecular weight TrkB-immunoreactive bands, highlighted by the rectangle.

In contrast, more favorable results were obtained when cells were first transfected and BfA treatment was initiated several hours later, followed by lysis 24 h post-transfection. Under these conditions, cells retained acceptable morphology and GFP fluorescence intensity while still producing detectable lower molecular weight TrkB bands consistent with immaturely glycosylated receptor forms (Figure 8A,C).

Western blot analysis supported the microscopy findings. The condition in which BfA treatment was applied after transfection and cells were lysed 24 h post-transfection produced the strongest overall TrkB signal together with the most prominent lower molecular weight TrkB-immunoreactive bands (Figure 8C). These approximately 100 kDa bands were consistent with molecular weight associated with immaturely glycosylated TrkB suggesting effective enrichment of immaturely processed receptor while maintaining sufficient protein expression and cell viability.

3.3 TrkB binding study validation on *Dianthus*

Several assay parameters were optimized prior to binding experiments in order to identify conditions compatible with fluorescence-based Dianthus measurements using TrkB-containing cell lysates.

3.3.1 Optimization of labeling strategy

The possibility of using TrkB fused with mCardinal was examined as this fluorescent protein has a far-red emission spectrum compatible with Dianthus' detectors. Despite the theoretical compatibility mCardinal did not produce detectable signal. In contrast, use of His-tagged lysates labelled with manufacturer's own dye produced stable fluorescence signals and enabled successful binding check measurements. Therefore, the His-tag RED-tris-NTA labeling approach was selected for further experiments (Figure 9A).

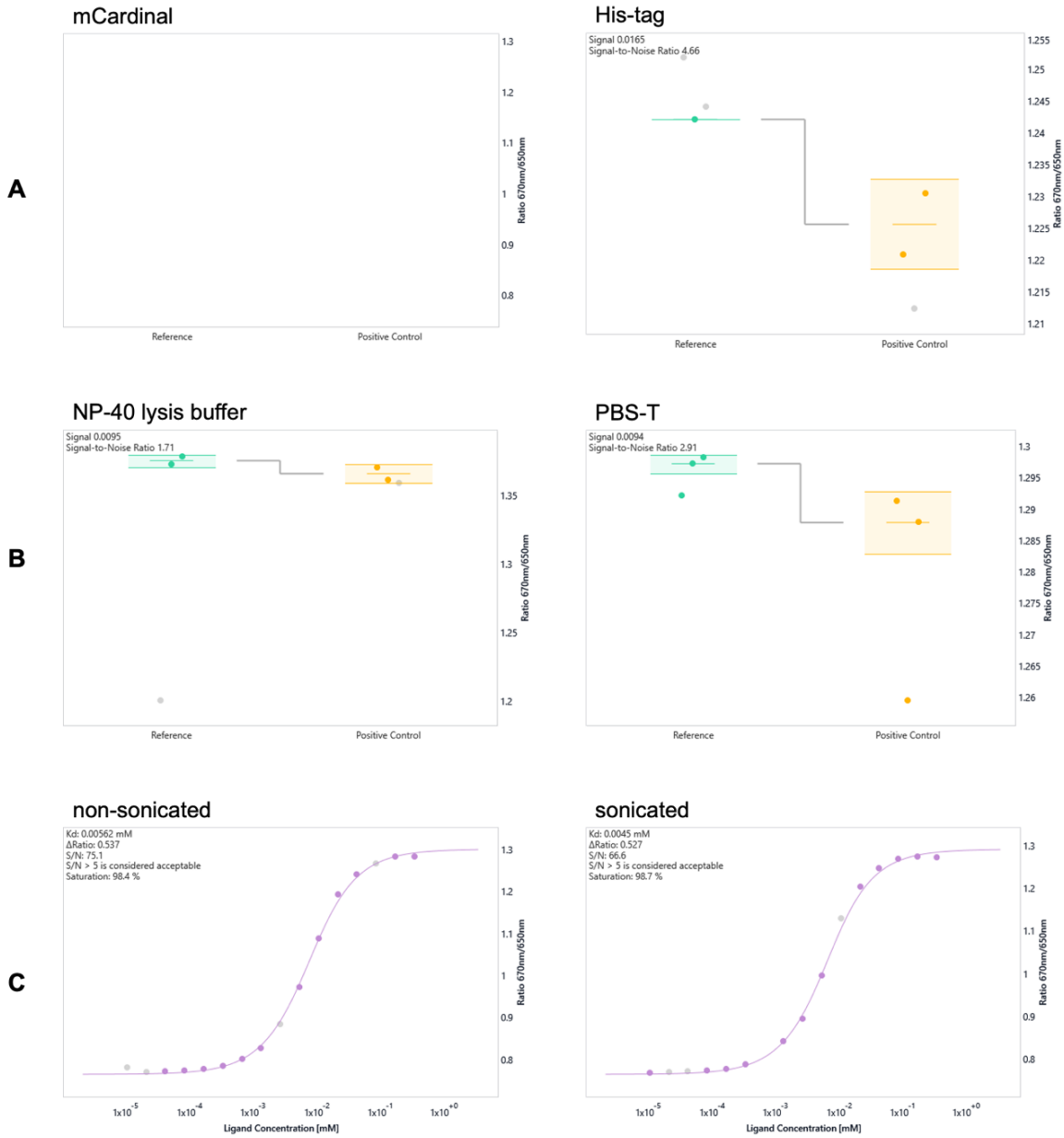

Figure 9. Sample optimization for Dianthus-based TrkB binding measurements. Representative Dianthus binding check measurements comparing different sample preparation conditions in HEK293T lysates expressing TrkB using LSD as a ligand. His-tag/RED-tris-NTA labeling, mechanical disruption in PBS-T and excluded sonication generally produced more robust and reproducible signal separation. **(A)** mCardinal-TrkB versus His-tagged TrkB labeled using RED-tris-NTA dye **(B)** NP-40 lysis buffer versus mechanical disruption in PBS-T and **(C)** sonicated versus non-sonicated samples.

3.3.2 Effect of lysis buffer composition

Because several NP-40 lysis buffer components are not either in the manufacturer's recommended limits or recommended at all as they may interfere with the labelling reaction, alternative mechanical lysis approaches using PBS-based buffer were investigated.

Both chemical and mechanical lysis approaches produced measurable fluorescence signals (Figure 9B). Mechanical disruption in PBS-T appeared to produce slightly improved

separation between positive control and reference samples compared with NP-40-based lysis, although signal-to-noise ratio (S/N) remained relatively modest under both conditions.

Because both approaches produced measurable fluorescence signals and the difference in assay performance was modest, existing NP-40 lysates were considered suitable for preliminary Dianthus assay development when diluted into PBS-T during labeling and measurement. Further optimization of lysis conditions was therefore postponed while the work focused on TrkB concentration estimation and receptor characterization.

3.3.3 Effect of sonication

Brief sonication was routinely used during lysate preparation to improve membrane receptor extraction. However, because NanoTemper generally does not recommend sonication when preparing samples for Dianthus screenings, its influence on assay performance and fluorescence behavior was evaluated.

Both conditions generated measurable binding curves; however, non-sonicated lysates produced more stable and reproducible measurements with lower apparent variability (Figure 9C). Sonicated samples showed increased scatter between individual measurement points and greater variability in curve fitting, suggesting that sonication may negatively affect fluorescence stability or sample homogeneity under these conditions. Therefore, non-sonicated lysates were preferred for subsequent Dianthus binding experiments.

3.3.4 Sample handling and plate preparation

Additional optimization focused on practical assay variables including mixing procedure, bubble formation, centrifugation, and plate handling. Because the Dianthus system is sensitive to optical artifacts, inadequate mixing or trapped air bubbles frequently reduced data quality.

Improved reproducibility was achieved by reverse pipetting, thorough mixing of samples, and brief centrifugation of plates prior to measurement. Use of recommended working volumes and careful handling of the thin-bottom 384-well assay plates further reduced technical variability.

Although these factors may appear minor, they had a clear impact on signal stability and curve quality during preliminary experiments.

3.4 Binding Affinity Screening of LSD to TrkB

During assay development, multiple exploratory binding affinity measurements were performed using different TrkB-containing lysates and selected ligands. One technically successful run is presented below to illustrate SpS, TRIC and well-scan profiles obtained during LSD–TrkB binding measurements using His-tagged wild-type and Y433F-mutated TrkB. According to NanoTemper's quality guidelines, ligand-associated responses are generally considered indicative of binding when the S/N exceeds 5 and the saturation level is greater than 50%, whereas saturation levels between 25–50% may indicate weaker binding interactions.

SpS measurements demonstrated sigmoidal fluorescence response patterns for both TrkB.wt and TrkB.Y433F lysates (Figure 11A,B). Together with relatively high S/Ns and saturation levels, these findings supported the presence of specific ligand-associated and concentration-dependent binding interactions.

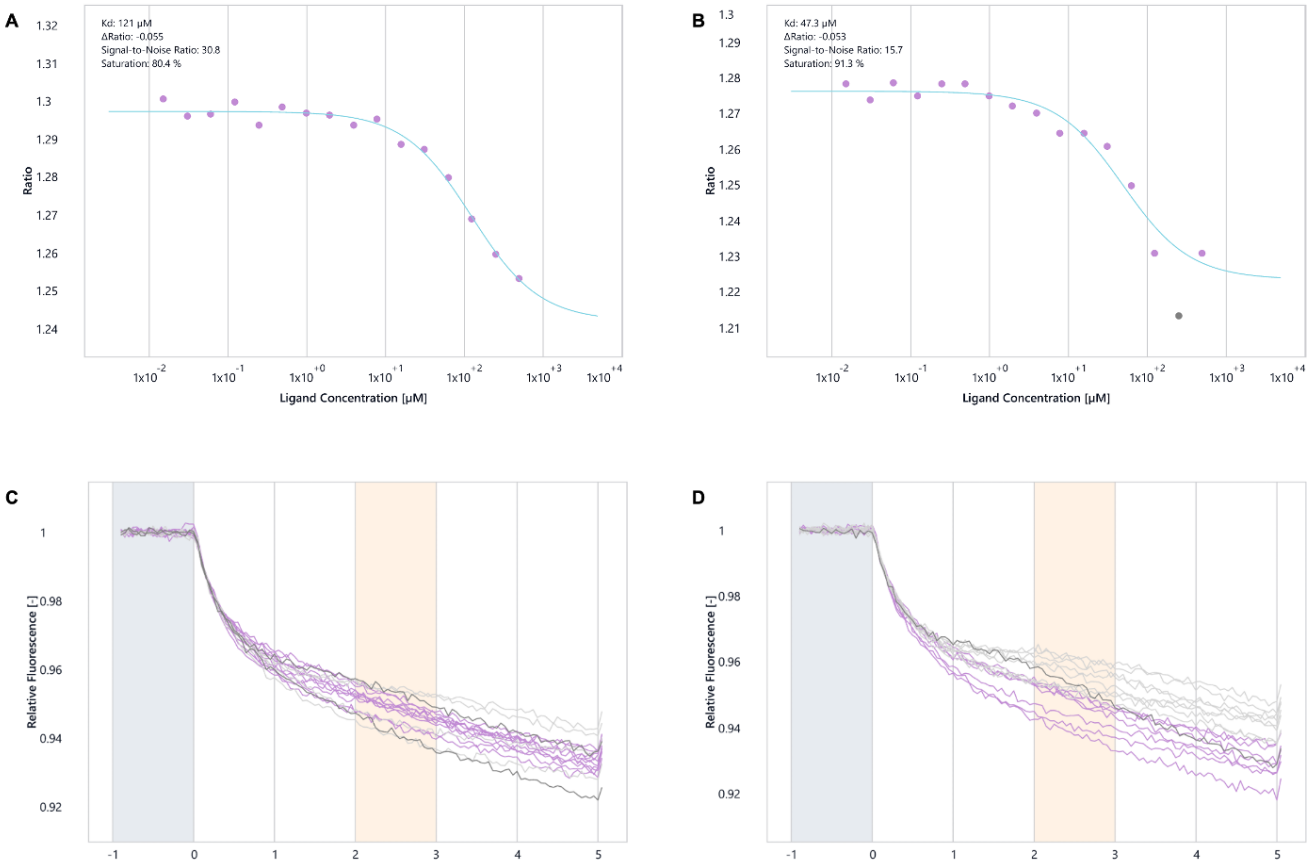

Figure 10. SpS and TRIC results from Dianthus binding affinity measurements using LSD as a ligand and lysates expressing either wild-type TrkB or Y433F mutant
(A) SpS measurement using lysates expressing TrkB.wt showing concentration-dependent fluorescence ratio changes following increasing LSD concentrations. (B) Corresponding SpS measurement using TrkB.Y433F lysates. (C) TRIC-trace obtained using lysates expressing TrkB.wt (D) Corresponding TRIC-trace obtained using TrkB.Y433F lysates.

TRIC-traces showed relatively reproducible concentration-dependent behavior across replicate measurements for both TrkB.wt and TrkB.Y433F lysates (Figure 11C,D). Increasing temperature induced progressive fluorescence decreases in both datasets, consistent with ligand-associated alterations in fluorescence behavior. Together with the corresponding SpS measurements, these TRIC fluorescence responses supported the presence of detectable ligand-associated interactions under lysate-based assay conditions.

Importantly, these measurements were performed before quantification of TrkB concentration in the lysates had been established. Consequently, receptor concentrations used for software-generated affinity fitting were based on preliminary estimates rather than experimentally validated concentrations. Therefore, apparent values obtained from these experiments should be interpreted cautiously and considered exploratory.

Dianthus performs automated 3D well scans to detect any anomalies in sample quality. Most wells demonstrated relatively uniform fluorescence distributions and stable scan profiles, indicating acceptable sample quality for measurement (Figure 11). Although occasional wells showed minor irregularities suggestive of optical artifacts or sample heterogeneity, the majority of measurements produced sufficiently stable fluorescence signals for further analysis.

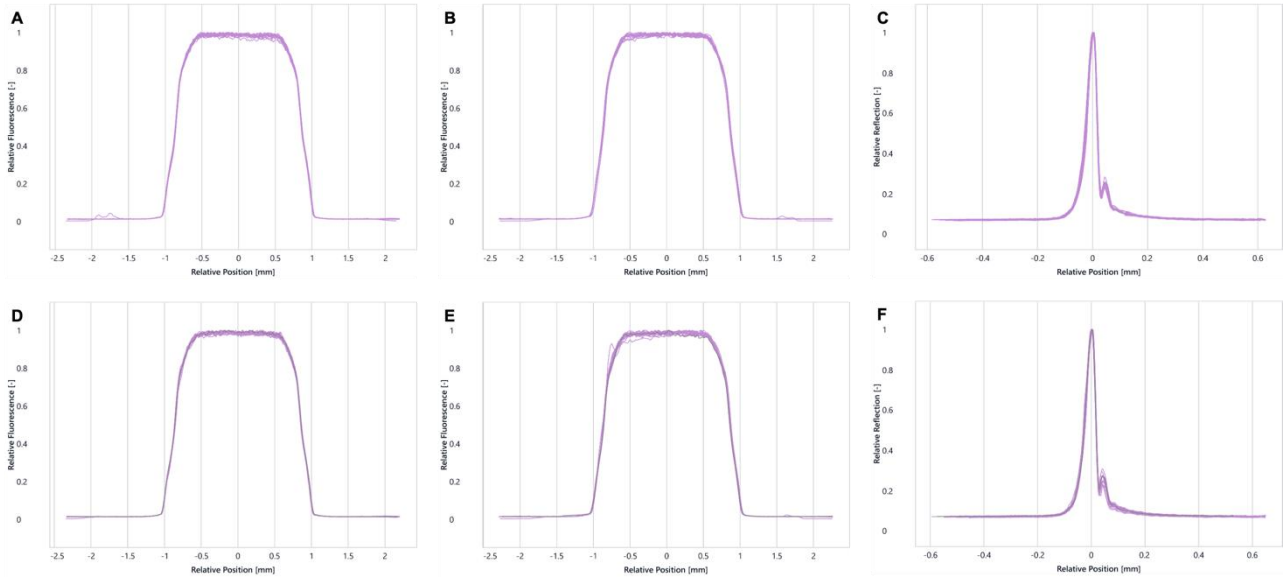

Figure 11. Well-scan profiles from Dianthus binding affinity measurements using LSD as a ligand and lysates expressing either wild-type TrkB or Y433F mutant.
(A-C) X-, Y-, and Z-scan profiles obtained from measurements using lysates expressing TrkB.wt.
(D-F) X-, Y-, and Z-scan profiles obtained from measurements using TrkB.Y433F lysates.
The scans demonstrated relatively uniform and stable signal profiles without major optical artifacts, supporting acceptable technical sample quality for Dianthus measurements.

Although acceptable technical signal quality could often be achieved, the resulting concentration–response curves frequently showed substantial variability, insufficient saturation and low S/Ns. Given the complexity of the lysate-based system and heterogeneous receptor populations, the observed signal quality and saturation behavior were considered sufficient for preliminary exploratory measurements but not for definitive quantitative affinity analysis.

Taken together, these results are consistent with previous studies reporting direct binding of psychedelics to TrkB and support the hypothesis that such interactions may contribute to their plasticity-promoting and antidepressant effects.

4 Discussion

4.1 Summary of Key Findings

The original aim of this study was to establish a Dianthus-based workflow for screening ligand interactions with TrkB and to evaluate whether classical psychedelics could be studied using this platform. However, in the course of the project it became evident that reliable ligand-binding measurements required substantial optimization and characterization of the experimental system itself. Consequently, the study evolved from a relatively straightforward ligand-screening project into a combined methodological and biological investigation focusing on receptor quantification, assay optimization, and TrkB heterogeneity.

The main findings of this work were threefold. First, HEK293T cells expressing TrkB contained sufficient receptor levels for preliminary binding studies, as confirmed by Western blotting and ELISA. Second, TrkB appeared as multiple molecular forms consistent with differential glycosylation states which could be modified by BfA treatment. Third, recurring ligand-associated and concentration-dependent responses were observed with LSD in Dianthus measurements. Together, these findings demonstrate both potential and the current limitations of lysate-based TrkB binding studies using the Dianthus platform.

4.2 TrkB expression and receptor heterogeneity

Reliable receptor quantification was an essential prerequisite for meaningful binding analysis. Initial concentration estimates were highly approximate, which complicated interpretation of Dianthus parameters. For this reason, independent quantification of TrkB abundance by Western blotting and ELISA represented an important step in establishing a more robust experimental framework.

In addition to confirming receptor expression, Western blotting consistently revealed multiple TrkB-immunoreactive bands. This observation is biologically plausible as TrkB displays considerable molecular heterogeneity, existing as multiple isoforms and in distinct glycosylation states (Andreska et al., 2020; Haapasalo et al., 2002; Liu et al., 2014; Rantamäki et al., 2011; Tessarollo & Yanpallewar, 2022). BfA treatment experiments

further supported this interpretation by shifting the band pattern toward lower molecular weight species consistent with immaturely glycosylated receptor forms.

These findings are particularly relevant for lysate-based binding assays, which do not measure a single homogeneous receptor population. Instead, the measured fluorescence signal likely reflects a complex mixture of mature membrane-associated receptors, immature intracellular forms, different isoforms, and potentially degraded protein fragments. Such heterogeneity may substantially influence ligand accessibility and assay performance, particularly when comparing structurally distinct ligands such as BDNF and small molecules.

4.3 Evaluation of the Dianthus platform

The Dianthus platform offers several practical advantages for receptor–ligand studies, including low sample consumption, relatively rapid workflow, compatibility with complex biological samples, and avoidance of receptor purification or immobilization (Hunter et al., 2025; Langer et al., 2022). These features are particularly attractive for membrane proteins such as TrkB, whose structural integrity may be altered during purification.

At the same time, the present work demonstrated that assay performance was highly sensitive to experimental variables including labeling strategy, sample preparation, buffer composition, and plate handling. Because the instrument had only recently been introduced to the laboratory, no established workflow for TrkB measurements was available at the start of the project. Consequently, a substantial proportion of the project focused on establishing reproducible experimental conditions rather than exclusively on hypothesis-driven ligand screening. However, such methodological optimization represents an essential component of early-stage assay implementation and provides an important foundation for future quantitative TrkB interaction studies.

Importantly, many of the identified challenges were not necessarily limitations of the Dianthus technology itself, but rather reflected the biological complexity of studying membrane receptor interactions in heterogeneous lysate systems.

4.4 LSD interaction with TrkB

Under optimized conditions, recurring concentration-dependent responses were observed with LSD in TrkB-containing lysates. Although ideal saturation curves were not

consistently achieved and technical variability remained, the repeated appearance of ligand-associated signal changes across multiple runs supports the conclusion that LSD interacts measurably with the assay system in a TrkB-dependent context.

These findings are consistent with previous reports proposing direct interactions between psychedelics and TrkB (Casarotto et al., 2021; Moliner et al., 2023) and further with the broader hypothesis that psychedelics may influence neuroplasticity-related pathways partly through modulation of TrkB signaling (Park & Poo, 2013; Vollenweider & Preller, 2020). TrkB activation has been strongly linked to neuronal plasticity, synaptic remodeling, and antidepressant responses (Coyle & Duman, 2003; Park & Poo, 2013).

Interpretation of the observed responses should nevertheless remain cautious because receptor concentrations were only approximately estimated during early measurements, and quantitative affinity calculations were therefore associated with substantial uncertainty. Rather, they should be interpreted as preliminary evidence supporting the feasibility of detecting psychedelic-associated TrkB interactions using a lysate-based fluorescence platform.

4.5 Limitations of the study

Several limitations should be acknowledged. First, the TrkB receptor was studied in an overexpression system rather than in native neuronal cells, which may promote non-physiological receptor clustering or spontaneous receptor dimerization, potentially influencing ligand accessibility and signaling behavior. Second, lysate-based samples contain heterogeneous protein mixtures that may affect both ligand accessibility and fluorescence measurements. Third, quantitative affinity estimates could not be robustly established because ideal saturation behavior was not consistently achieved. Finally, functional downstream signaling responses were not assessed in the present work.

Despite these limitations, the study successfully identified critical variables influencing assay performance and generated preliminary biologically relevant observations.

4.6 Future directions

Future work should focus on refining the assay system to improve receptor homogeneity, signal stability, and quantitative curve fitting. Alternative cellular models, including systems with more physiological TrkB processing, may be beneficial.

An important future objective would be to further characterize the functional relevance of distinct TrkB glycosylation states. One potential future approach would involve enrichment or separation of differently glycosylated receptor populations using lectin-based methods such as concanavalin A affinity isolation. Concanavalin A binds to α-D-mannose and α-D-glucose residues on glycoproteins and has been widely used for isolating glycoproteins (Lam et al., 2012). Since receptor maturation and post-translational processing are known to influence Trk receptor trafficking and signaling properties (Andreska et al., 2020; Liu et al., 2014), such experiments could help clarify whether immaturely and maturely glycosylated TrkB populations differ in ligand accessibility, phosphorylation, or responsiveness to BDNF, antidepressants, and psychedelics. This may provide additional insight into how receptor maturation state influences TrkB-mediated signaling and ligand interactions.

From a translational perspective, an especially important future question is whether TrkB-modulating effects of psychedelics occur at concentrations separable from those producing hallucinogenic 5-HT2A-mediated effects (Vargas et al., 2021; Vollenweider & Preller, 2020). If such separation is achievable, it could support development of next-generation rapid-acting antidepressants with improved safety and tolerability.

4.7 Conclusion

This study demonstrates that the Dianthus platform is a promising tool for investigating receptor-ligand interactions in complex biological samples, although careful optimization of both biological and technical parameters is required. Quantification and characterization of receptor preparations proved essential for meaningful assay interpretation, particularly given the heterogeneous receptor populations present in lysate-based systems. Recurring LSD-associated responses supported the feasibility of detecting psychedelic-associated TrkB interactions using lysate-based fluorescence assays. Together, these findings provide a practical foundation for future quantitative studies of TrkB-targeting compounds and contribute to the broader understanding of neuroplasticity-related antidepressant mechanisms. Importantly, the present work also established practical methodological groundwork for future quantitative studies using the Dianthus platform in TrkB-related ligand screening.

Acknowledgements

I would like to sincerely thank my supervisors, Docent Vadim Le Joncour and Professor Eero Castrén, for their guidance, expertise, patience, and support throughout this project. Thank you for giving me the opportunity to work with you and for introducing me to the world of neuroplasticity research – it truly was a dream come true. Writing this thesis turned out to be a much longer and more complicated journey than originally planned, and I am especially grateful for your understanding and encouragement during the more difficult phases along the way.

In addition, I would like to thank everyone in the Trophins lab and the Neuroscience Center for all the advice, help, discussions, and shared moments in the lab. I learned an enormous amount during this project, not only about research work but also about life in general. I am especially grateful for the support and understanding I received during a particularly difficult period of my life. Many people at the lab saw me at my lowest, yet I was consistently met with patience, kindness, and encouragement. Vadim, Italo Brothers, your support and friendship mean more to me than I can properly express, and I will always be deeply grateful for meeting you. I can honestly say that the time I spent working with you was one of the most meaningful periods of my life.

I would also like to express my appreciation to the Sigrid Jusélius Foundation for the grant that made it possible for me to continue working in the lab longer than originally planned and allowed me to fully focus on the project during an important stage of the thesis work.

Finally, I want to thank my family and friends for their support, patience and love throughout the thesis process and these overwhelming years. Completing this thesis often felt impossible, and I would not have made it here without the people around me believing in me even when I struggled to believe in myself. To all my loved ones who patiently tolerated my prolonged disappearance into thesis-writing chaos: thank you. I fully intend to start answering messages, picking up calls, and existing socially again after this.

SSDGM,

Abbreviations

5-HT_{2A} — Serotonin 2A receptor

Akt — Protein kinase B

BfA — Brefeldin A

BDNF — Brain-derived neurotrophic factor

BSA — Bovine serum albumin

CNS — Central nervous system

DMEM — Dulbecco's Modified Eagle Medium

DNA — Deoxyribonucleic acid

ECD — extracellular domain

ECL — Enhanced chemiluminescence

ELISA — Enzyme-linked immunosorbent assay

ERK — Extracellular signal-regulated kinase

FBS — Fetal bovine serum

GAPDH — Glyceraldehyde 3-phosphate dehydrogenase

GFP — Green fluorescent protein

HEK293T — Human embryonic kidney 293T cells

HRP — Horseradish peroxidase

LSD — Lysergic acid diethylamide

LTP — Long-term potentiation

LTD — Long-term depression

MAPK — Mitogen-activated protein kinase

MST — Microscale thermophoresis

MTT — 3-(4, 5-dimethylthiazolyl-2)-2, 5-diphenyltetrazolium bromide

mTOR — Mechanistic target of rapamycin

NP-40 — Nonidet P-40 detergent

OD — Optical density

PBS — Phosphate-buffered saline

PBS-T — Phosphate-buffered saline with Tween® 20

PI3K — Phosphoinositide 3-kinase

PLCγ — Phospholipase C gamma

PVDF — Polyvinylidene fluoride

RAAD — Rapid-acting antidepressant

RcTrkB — recombinant human TrkB Fc chimera protein

RT — Room temperature

SDS–PAGE — Sodium dodecyl sulfate polyacrylamide gel electrophoresis

S/N — Signal-to-noise ratio

SPR — Surface plasmon resonance

SpS — Spectral shift

SSRI — Selective serotonin reuptake inhibitor

TBS-T — Tris-buffered saline with Tween® 20

TMB — Tetramethylbenzidine

TRIC — Temperature-related intensity change

TrkB — Neurotrophic tyrosine receptor kinase 2

References

Albert, P.R. 2019. Adult neuroplasticity: A new “cure” for major depression? *J. Psychiatry Neurosci.* 44:147–150. doi:10.1503/jpn.190072.

Andreska, T., P. Lüningschrör, and M. Sendtner. 2020. Regulation of TrkB cell surface expression—a mechanism for modulation of neuronal responsiveness to brain-derived neurotrophic factor. *Cell Tissue Res.* 382:5–14. doi:10.1007/s00441-020-03224-7.

Antila, H., H. Autio, L. Turunen, K. Harju, P. Tammela, K. Wennerberg, J. Yli-Kauhaluoma, H.J. Huttunen, E. Castrén, and T. Rantamäki. 2014. Utilization of in situ ELISA method for examining Trk receptor phosphorylation in cultured cells. *J. Neurosci. Methods*. 222:142–146. doi:10.1016/j.jneumeth.2013.11.001.

Autry, A.E., and L.M. Monteggia. 2012. Brain-Derived Neurotrophic Factor and Neuropsychiatric Disorders. *Pharmacol. Rev.* 64:238–258. doi:10.1124/pr.111.005108.

Berman, R.M., A. Cappiello, A. Anand, D.A. Oren, G.R. Heninger, D.S. Charney, and J.H. Krystal. 2000. Antidepressant effects of ketamine in depressed patients. *Biol. Psychiatry*. 47:351–354. doi:10.1016/S0006-3223(99)00230-9.

Biojone, C., C. Cannarozzo, N. Seiffert, C.R.A.F. Diniz, C.A. Brunello, E. Castrén, and P. Casarotto. 2024. Mutation in the TRKB Cholesterol Recognition Site that blocks Antidepressant Binding does not Influence the Basal or BDNF-Stimulated Activation of TRKB. *Cell. Mol. Neurobiol.* 44:4. doi:10.1007/s10571-023-01438-1.

Bosshart, H., P. Straehl, B. Berger, and E.G. Berger. 1991. Brefeldin A induces endoplasmic reticulum-associated O-glycosylation of galactosyltransferase. *J. Cell. Physiol.* 147:149–156. doi:10.1002/jcp.1041470119.

Brunello, C.A., C. Cannarozzo, and E. Castrén. 2024. Rethinking the role of TRKB in the action of antidepressants and psychedelics. *Trends Neurosci.* 47:865–874. doi:10.1016/j.tins.2024.08.011.

Cannarozzo, C., A. Rubiolo, P. Casarotto, and E. Castrén. 2023. Ketamine and its metabolite 2 *R* ,6 *R* -hydroxynorketamine promote ocular dominance plasticity and release tropomyosin-related kinase B from inhibitory control without reducing perineuronal nets enwrapping parvalbumin interneurons. *Eur. J. Neurosci.* 57:940–950. doi:10.1111/ejn.15929.

Carhart-Harris, R.L., and G.M. Goodwin. 2017. The Therapeutic Potential of Psychedelic Drugs: Past, Present, and Future. *Neuropsychopharmacology*. 42:2105–2113. doi:10.1038/npp.2017.84.

Casarotto, P.C., M. Girych, S.M. Fred, V. Kovaleva, R. Moliner, G. Enkavi, C. Biojone, C. Cannarozzo, M.P. Sahu, K. Kaurinkoski, C.A. Brunello, A. Steinzeig, F. Winkel, S. Patil, S. Vestring, T. Serchov, C.R.A.F. Diniz, L. Laukkanen, I. Cardon, H. Antila, T. Rog, T.P. Piepponen, C.R. Bramham, C. Normann, S.E. Lauri, M. Saarma, I. Vattulainen, and E. Castrén. 2021. Antidepressant drugs act by directly binding to TRKB neurotrophin receptors. *Cell*. 184:1299-1313.e19. doi:10.1016/j.cell.2021.01.034.

Castanheira, S., C.V. Gomes, J. Bicker, and A. Fortuna. 2025. Novel mechanisms underlying rapid-acting antidepressants: ketamine-like compounds, neurosteroid GABAkines, and psychedelics. *Drug Discov. Today*. 30:104371. doi:10.1016/j.drudis.2025.104371.

Castrén, E. 2005. Is mood chemistry? *Nat. Rev. Neurosci.* 6:241–246. doi:10.1038/nrn1629.

Castrén, E., and H. Antila. 2017. Neuronal plasticity and neurotrophic factors in drug responses. *Mol. Psychiatry*. 22:1085–1095. doi:10.1038/mp.2017.61.

Castrén, E., and L.M. Monteggia. 2021. Brain-Derived Neurotrophic Factor Signaling in Depression and Antidepressant Action. *Biol. Psychiatry*. 90:128–136. doi:10.1016/j.biopsych.2021.05.008.

Chao, M.V. 2003. Neurotrophins and their receptors: A convergence point for many signalling pathways. *Nat. Rev. Neurosci.* 4:299–309. doi:10.1038/nrn1078.

Cipriani, A., T.A. Furukawa, G. Salanti, A. Chaimani, L.Z. Atkinson, Y. Ogawa, S. Leucht, H.G. Ruhe, E.H. Turner, J.P.T. Higgins, M. Egger, N. Takeshima, Y. Hayasaka, H. Imai, K. Shinohara, A. Tajika, J.P.A. Ioannidis, and J.R. Geddes. 2018. Comparative efficacy and acceptability of 21 antidepressant drugs for the acute treatment of adults with major depressive disorder: a systematic review and network meta-analysis. *The Lancet*. 391:1357–1366. doi:10.1016/S0140-6736(17)32802-7.

Coyle, J.T., and R.S. Duman. 2003. Finding the Intracellular Signaling Pathways Affected by Mood Disorder Treatments. *Neuron*. 38:157–160. doi:10.1016/S0896-6273(03)00195-8.

Duman, R.S., G.K. Aghajanian, G. Sanacora, and J.H. Krystal. 2016. Synaptic plasticity and depression: new insights from stress and rapid-acting antidepressants. *Nat. Med.* 22:238–249. doi:10.1038/nm.4050.

Duman, R.S., and L.M. Monteggia. 2006. A Neurotrophic Model for Stress-Related Mood Disorders. *Biol. Psychiatry*. 59:1116–1127. doi:10.1016/j.biopsych.2006.02.013.

Enkavi, G., M. Girych, R. Moliner, I. Vattulainen, and E. Castrén. 2024. TrkB transmembrane domain: bridging structural understanding with therapeutic strategy. *Trends Biochem. Sci.* 49:445–456. doi:10.1016/j.tibs.2024.02.001.

Fuchs, E., and G. Flügge. 2014. Adult Neuroplasticity: More Than 40 Years of Research. *Neural Plast.* 2014:1–10. doi:10.1155/2014/541870.

GBD 2019 Mental Disorders Collaborators. 2022. Global, regional, and national burden of 12 mental disorders in 204 countries and territories, 1990–2019: a systematic analysis for the Global Burden of Disease Study 2019. *Lancet Psychiatry*. 9:137–150. doi:10.1016/S2215-0366(21)00395-3.

Haapasalo A., I. Sipola, K. P. Larsson, K. E.O. Åkerman, P. Stoilov, S. Stamm, G. Wong, and E. Castrén. 2002. Regulation of TRKB Surface Expression by Brain-derived Neurotrophic Factor and Truncated TRKB Isoforms. *J. Biol. Chem.*, 277(45), 43160–43167. https://doi.org/10.1074/jbc.m205202200Haniu, M., J. Talvenheimo, J. Le, V. Katta, A. Welcher, and M.F. Rohde. 1995. Extracellular Domain of Neurotrophin Receptor trkB: Disulfide Structure, N-Glycosylation Sites, and Ligand Binding. *Arch. Biochem. Biophys.* 322:256–264. doi:10.1006/abbi.1995.1460.

Harmer, C.J., R.S. Duman, and P.J. Cowen. 2017. How do antidepressants work? New perspectives for refining future treatment approaches. *Lancet Psychiatry*. 4:409–418. doi:10.1016/S2215-0366(17)30015-9.

Hirschfeld, R.M.A. 2000. History and Evolution of the Monoamine Hypothesis of Depression. *J Clin Psychiatry*. 61:4–6.

Huang, E.J., and L.F. Reichardt. 2001. Neurotrophins: Roles in Neuronal Development and Function. *Annu. Rev. Neurosci.* 24:677–736. doi:10.1146/annurev.neuro.24.1.677.

Huang, E.J., and L.F. Reichardt. 2003. Trk Receptors: Roles in Neuronal Signal Transduction. *Annu. Rev. Biochem.* 72:609–642. doi:10.1146/annurev.biochem.72.121801.161629.

Hunter, C.E., E. Pohl, and S. Freitag-Pohl. 2025. High-throughput investigation of macromolecular interactions for drug development using spectral shift technology. *Biophys. Rev.* 17:959–980. doi:10.1007/s12551-025-01359-x.

Jerabek-Willemsen, M., T. André, R. Wanner, H.M. Roth, S. Duhr, P. Baaske, and D. Breitsprecher. 2014. MicroScale Thermophoresis: Interaction analysis and beyond. *J. Mol. Struct.* 1077:101–113. doi:10.1016/j.molstruc.2014.03.009.

Kraus, C., E. Castrén, S. Kasper, and R. Lanzenberger. 2017. Serotonin and neuroplasticity – Links between molecular, functional and structural pathophysiology in depression. *Neurosci. Biobehav. Rev.* 77:317–326. doi:10.1016/j.neubiorev.2017.03.007.

Kuczewski, N., C. Porcher, V. Lessmann, I. Medina, and J.-L. Gaiarsa. 2009. Activity-Dependent Dendritic Release of BDNF and Biological Consequences. *Mol. Neurobiol.* 39:37–49. doi:10.1007/s12035-009-8050-7.

Lam, M.P.Y., E. Lau, X. Liu, J. Li, and I.K. Chu. 2012. Sample preparation for glycoproteins. *In* Comprehensive Sampling and Sample Preparation. J. Pawliszyn, editor. Academic Press, Oxford. 307–322.doi:10.1016/B978-0-12-381373-2.00085-5

Langer, A., A. Lüdecke, T. Bartoschik, O. Cehlar, S. Duhr, P. Baaske, and W. Streicher. 2022. A New Spectral Shift-Based Method to Characterize Molecular Interactions. *ASSAY Drug Dev. Technol.* 20:83–94. doi:10.1089/adt.2021.133.

Liu, B., J. Liu, M. Wang, Y. Zhang, and L. Li. 2017. From Serotonin to Neuroplasticity: Evolvement of Theories for Major Depressive Disorder. *Front. Cell. Neurosci.* 11:305. doi:10.3389/fncel.2017.00305.

Liu, X., O. Obianyo, C.B. Chan, J. Huang, S. Xue, J.J. Yang, F. Zeng, M. Goodman, and K. Ye. 2014. Biochemical and Biophysical Investigation of the Brain-derived Neurotrophic Factor Mimetic 7,8-Dihydroxyflavone in the Binding and Activation of the TrkB Receptor. *J. Biol. Chem.* 289:27571–27584. doi:10.1074/jbc.M114.562561.

López-Méndez, B., S. Uebel, L.P. Lundgren, and A. Sedivy. 2021. Microscale Thermophoresis and additional effects measured in NanoTemper Monolith instruments. *Eur. Biophys. J.* 50:653–660. doi:10.1007/s00249-021-01529-1.

Ly, C., A.C. Greb, L.P. Cameron, J.M. Wong, E.V. Barragan, P.C. Wilson, K.F. Burbach, S. Soltanzadeh Zarandi, A. Sood, M.R. Paddy, W.C. Duim, M.Y. Dennis, A.K. McAllister, K.M. Ori-McKenney, J.A. Gray, and D.E. Olson. 2018. Psychedelics Promote Structural and Functional Neural Plasticity. *Cell Rep.* 23:3170–3182. doi:10.1016/j.celrep.2018.05.022.

Ly, C., A.C. Greb, M.V. Vargas, W.C. Duim, A.C.G. Grodzki, P.J. Lein, and D.E. Olson. 2021. Transient Stimulation with Psychoplastogens Is Sufficient to Initiate Neuronal Growth. *ACS Pharmacol. Transl. Sci.* 4:452–460. doi:10.1021/acsptsci.0c00065.

Ma, Z., T. Zang, S.G. Birnbaum, Z. Wang, J.E. Johnson, C.-L. Zhang, and L.F. Parada. 2017. TrkB dependent adult hippocampal progenitor differentiation mediates sustained ketamine antidepressant response. *Nat. Commun.* 8:1668. doi:10.1038/s41467-017-01709-8.

Malhi, G.S., and J.J. Mann. 2018. Depression. *The Lancet*. 392:2299–2312. doi:10.1016/S0140-6736(18)31948-2.

Manji, H.K., W.C. Drevets, and D.S. Charney. 2001. The cellular neurobiology of depression. *Nat. Med.* 7:541–547. doi:10.1038/87865.

McAllister, A.K., L.C. Katz, and D.C. Lo. 1999. Neurotrophins and synaptic plasticity. *Annu. Rev. Neurosci.* 22:295–318.

Mitre, M., A. Mariga, and M.V. Chao. 2017. Neurotrophin signalling: novel insights into mechanisms and pathophysiology. *Clin. Sci.* 131:13–23. doi:10.1042/CS20160044.

Moliner, R., M. Girych, C.A. Brunello, V. Kovaleva, C. Biojone, G. Enkavi, L. Antenucci, E.F. Kot, S.A. Goncharuk, K. Kaurinkoski, M. Kuutti, S.M. Fred, L.V. Elsilä, S. Sakson, C. Cannarozzo, C.R.A.F. Diniz, N. Seiffert, A. Rubiolo, H. Haapaniemi, E. Meshi, E. Nagaeva, T. Öhman, T. Róg, E. Kankuri, M. Vilar, M. Varjosalo, E.R. Korpi, P. Permi, K.S. Mineev, M. Saarma, I. Vattulainen, P.C. Casarotto, and E. Castrén. 2023. Psychedelics promote plasticity by directly binding to BDNF receptor TrkB. *Nat. Neurosci.* 26:1032–1041. doi:10.1038/s41593-023-01316-5.

Moremen, K.W., M. Tiemeyer, and A.V. Nairn. 2012. Vertebrate protein glycosylation: diversity, synthesis and function. *Nat. Rev. Mol. Cell Biol.* 13:448–462. doi:10.1038/nrm3383.

Mulinari, S. 2012. Monoamine Theories of Depression: Historical Impact on Biomedical Research. *J. Hist. Neurosci.* 21:366–392. doi:10.1080/0964704X.2011.623917.

Nestler, E.J., M. Barrot, R.J. DiLeone, A.J. Eisch, S.J. Gold, and L.M. Monteggia. 2002. Neurobiology of Depression Review. *Neuron*. 34:13–25.

Nibuya, M., S. Morinobu, and R. Duman. 1995. Regulation of BDNF and trkB mRNA in rat brain by chronic electroconvulsive seizure and antidepressant drug treatments. *J. Neurosci.* 15:7539–7547. doi:10.1523/JNEUROSCI.15-11-07539.1995.

Park, H., and M. Poo. 2013. Neurotrophin regulation of neural circuit development and function. *Nat. Rev. Neurosci.* 14:7–23. doi:10.1038/nrn3379.

Pittenger, C., and R.S. Duman. 2008. Stress, Depression, and Neuroplasticity: A Convergence of Mechanisms. *Neuropsychopharmacology*. 33:88–109. doi:10.1038/sj.npp.1301574.

Rantamäki, T., Hendolin, P., Kankaanpää, A., Mijatovic, J., Piepponen, P., Domenici, E., Chao, M. V., Männistö, P. T., & Castrén, E. (2007). Pharmacologically diverse antidepressants rapidly activate brain-derived neurotrophic factor receptor TrkB and induce phospholipase-Cgamma signaling pathways in mouse brain. Neuropsychopharmacology : official publication of the American College of Neuropsychopharmacology, 32(10), 2152–2162. doi:10.1038/sj.npp.1301345

Rantamäki, T., L. Vesa, H. Antila, A. Di Lieto, P. Tammela, A. Schmitt, K.-P. Lesch, M. Rios, and E. Castrén. 2011. Antidepressant Drugs Transactivate TrkB Neurotrophin Receptors in the Adult Rodent Brain Independently of BDNF and Monoamine Transporter Blockade. *PLoS ONE*. 6:e20567. doi:10.1371/journal.pone.0020567.

Rush, A.J., M.H. Trivedi, S.R. Wisniewski, A.A. Nierenberg, J.W. Stewart, D. Warden, G. Niederehe, M.E. Thase, P.W. Lavori, B.D. Lebowitz, P.J. McGrath, J.F. Rosenbaum, and

H.A. Sackeim. 2006. Acute and Longer-Term Outcomes in Depressed Outpatients Requiring One or Several Treatment Steps: A STAR*D Report. *Am J Psychiatry*. 163(11), 1905–1917. doi:10.1176/ajp.2006.163.11.1905

Saarelainen, T., P. Hendolin, G. Lucas, E. Koponen, M. Sairanen, E. MacDonald, K. Agerman, A. Haapasalo, H. Nawa, R. Aloyz, P. Ernfors, and E. Castrén. 2003. Activation of the TrkB Neurotrophin Receptor Is Induced by Antidepressant Drugs and Is Required for Antidepressant-Induced Behavioral Effects. *J. Neurosci.* 23:349–357. doi:10.1523/JNEUROSCI.23-01-00349.2003.

Saelens, J., A. Gramser, V. Watzal, C.A. Zarate, R. Lanzenberger, and C. Kraus. 2025. Relative effectiveness of antidepressant treatments in treatment-resistant depression: a systematic review and network meta-analysis of randomized controlled trials. *Neuropsychopharmacology*. 50:913–919. doi:10.1038/s41386-024-02044-5.

Santomauro, D.F., A.M. Mantilla Herrera, J. Shadid, P. Zheng, C. Ashbaugh, D.M. Pigott, C. Abbafati, C. Adolph, J.O. Amlag, A.Y. Aravkin, B.L. Bang-Jensen, G.J. Bertolacci, S.S. Bloom, R. Castellano, E. Castro, S. Chakrabarti, J. Chattopadhyay, R.M. Cogen, J.K. Collins, X. Dai, W.J. Dangel, C. Dapper, A. Deen, M. Erickson, S.B. Ewald, A.D. Flaxman, J.J. Frostad, N. Fullman, J.R. Giles, A.Z. Giref, G. Guo, J. He, M. Helak, E.N. Hulland, B. Idrisov, A. Lindstrom, E. Linebarger, P.A. Lotufo, R. Lozano, B. Magistro, D.C. Malta, J.C. Månsson, F. Marinho, A.H. Mokdad, L. Monasta, P. Naik, S. Nomura, J.K. O'Halloran, S.M. Ostroff, M. Pasovic, L. Penberthy, R.C. Reiner Jr, G. Reinke, A.L.P. Ribeiro, A. Sholokhov, R.J.D. Sorensen, E. Varavikova, A.T. Vo, R. Walcott, S. Watson, C.S. Wiysonge, B. Zigler, S.I. Hay, T. Vos, C.J.L. Murray, H.A. Whiteford, and A.J. Ferrari. 2021. Global prevalence and burden of depressive and anxiety disorders in 204 countries and territories in 2020 due to the COVID-19 pandemic. *The Lancet*. 398:1700–1712. doi:10.1016/S0140-6736(21)02143-7.

Schinder, A., and M. Poo. 2000. The neurotrophin hypothesis for synaptic plasticity. *Trends Neurosci.* 23:639–645. doi:10.1016/S0166-2236(00)01672-6.

Stanley, P. 2011. Golgi Glycosylation. *Cold Spring Harbor Perspectives in Biology*, *3*(4), a005199–a005199. doi:10.1101/cshperspect.a005199

Tessarollo, L., and S. Yanpallewar. 2022. TrkB Truncated Isoform Receptors as Transducers and Determinants of BDNF Functions. *Front. Neurosci.* 16:847572. doi:10.3389/fnins.2022.847572.

Thoenen, H. 1995. Neurotrophins and Neuronal Plasticity. *Science*. 270:593–598. doi:10.1126/science.270.5236.593.

Vargas, M. V., R. Meyer, A. A. Avanes, M. Rus, and D. E. Olson. 2021. Psychedelics and Other Psychoplastogens for Treating Mental Illness. *Frontiers in Psychiatry*, *12*. doi:10.3389/fpsyt.2021.727117

Vesa, J., A. Krüttgen, and E.M. Shooter. 2000. p75 Reduces TrkB Tyrosine Autophosphorylation in Response to Brain-derived Neurotrophic Factor and Neurotrophin 4/5. *J. Biol. Chem.* 275:24414–24420. doi:10.1074/jbc.M001641200.

Wang, C.S., E.T. Kavalali, and L.M. Monteggia. 2022. BDNF signaling in context: From synaptic regulation to psychiatric disorders. *Cell*. 185:62–76. doi:10.1016/j.cell.2021.12.003.

Zhao, L., A.-L. Sheng, S.-H. Huang, Y.-X. Yin, B. Chen, X.-Z. Li, Y. Zhang, and Z.-Y. Chen. 2009. Mechanism underlying activity-dependent insertion of TrkB into the neuronal surface. *J. Cell Sci.* 122:3123–3136. doi:10.1242/jcs.047712.

Appendices

Appendix 1 AI Use Declaration

Generative artificial intelligence (AI) was used as a supportive tool during the preparation of this thesis in accordance with the University of Turku guidelines.

Tool name and version: OpenAI ChatGPT (GPT-5.3)

AI was used as a supportive tool in:

- Checking grammar and improving the clarity of the text
- Refining the academic tone and improving readability
- Conceptual visualization of selected schematic figures (Figures 2 and 3)

AI-generated suggestions were used as a starting point or for refinement only. All generated content was critically evaluated, edited, and finalized by the author. All source material and scientific content were selected and provided to AI by the author. Schematic figures were designed and finalized by the author, with AI assisting in visualization only.
All scientific content was verified against peer-reviewed literature and original sources. AI-generated content was checked for accuracy and consistency with cited references. The author is fully responsible for all content and interpretations presented in this thesis.